

ARTICLE



BAP18 facilitates CTCF-mediated chromatin accessible to regulate enhancer activity in breast cancer

Ge Sun¹, Yuntao Wei², Baosheng Zhou¹, Manlin Wang¹, Ruina Luan¹, Yu Bai¹, Hao Li¹, Shan Wang¹, Dantong Zheng¹, Chunyu Wang¹, Shengli Wang¹, Kai Zeng¹, Shuchang Liu¹, Lin Lin¹, Mingcong He¹, Qiang Zhang² and Yue Zhao¹ 

© The Author(s), under exclusive licence to ADMC Associazione Differenziamento e Morte Cellulare 2023

The estrogen receptor alpha (ERα) signaling pathway is a crucial target for ERα-positive breast cancer therapeutic strategies. Coregulators and other transcription factors cooperate for effective ERα-related enhancer activation. Recent studies demonstrate that the transcription factor CTCF is essential to participate in ERα/E2-induced enhancer transactivation. However, the mechanism of how CTCF is achieved remains unknown. Here, we provided evidence that BAP18 is required for CTCF recruitment on ERα-enriched enhancers, facilitating CTCF-mediated chromatin accessibility to promote enhancer RNAs transcription. Consistently, GRO-seq demonstrates that the enhancer activity is positively correlated with BAP18 enrichment. Furthermore, BAP18 interacts with SMARCA1/BPTF to accelerate the recruitment of CTCF to ERα-related enhancers. Interestingly, BAP18 is involved in chromatin accessibility within enhancer regions, thereby increasing enhancer transactivation and enhancer-promoter looping. BAP18 depletion increases the sensitivity of anti-estrogen and anti-enhancer treatment in MCF7 cells. Collectively, our study indicates that BAP18 coordinates with CTCF to enlarge the transactivation of ERα-related enhancers, providing a better understanding of BAP18/CTCF coupling chromatin remodeling and E-P looping in the regulation of enhancer transcription.

Cell Death & Differentiation (2023) 30:1260–1278; <https://doi.org/10.1038/s41418-023-01135-y>

INTRODUCTION

Cancer cells evolve to resist targeted therapies, which is a persistent issue in cancer treatment, particularly in breast cancer [1–3]. More than two-thirds of all breast cancers possess estrogen receptor alpha (ERα) positive and frequently respond to endocrine treatment, including tamoxifen, fulvestrant, and aromatase inhibitors (AI), which interfere with E2/ERα signaling [4, 5]. Women with ERα-positive breast cancer have been treated with AIs as a first-line treatment strategy [6]. Compared to tamoxifen, AIs therapies have higher clinical efficacy, longer disease-free survival, and fewer serious side effects [7]. Despite the fact that AI therapy reduces tumor recurrence by almost half, about one-quarter of patients fail to respond to AI therapy. Approximately 30% of patients develop tumor recurrence within ten years [8, 9]. Several molecular mechanisms have been identified as contributing to AI resistance, including mutations of CYP19A1, mutations of the ERα ligand-binding domain, compensatory activation of signaling (such as GPCR, PI3K/AKT/mTOR, and RAF/MEK/ERK), transcription reprogramming, and altered epigenetic modifications [10–13]. However, the mechanism of resistance to AI treatment is emerging. Recent studies suggest an essential role in ERα-related transactivation reprogramming in intrinsic endocrine resistance [14, 15]. There has been a significant increase in the activation of enhancers and the sustained expression of their target genes during endocrine treatment, leading to a shift from medication susceptibility to resistance in tumor cells [16, 17].

Despite these recent advances, the mechanisms responsible for AI resistance remain elusive.

ERα, the driving transcription factor of the luminal subtype of breast cancer, is a nuclear receptor that combines chromatin to regulate the transcription of its target genes, ultimately promoting cell proliferation and metastasis [18]. ChIP-seq analysis of ERα reveals that most binding sites are localized on distal enhancers and generate noncoding enhancer RNAs (eRNAs) of target genes, which dictates cell growth and the endocrine response in breast cancer [19–21]. Other transcription factors, coactivators, and pioneer factors are essential for enhancer activation [22, 23]. It has been demonstrated that global reprogramming of estrogen-responsive genes can alter endocrine sensitivity, contributing to the cancer process and endocrine resistance [24]. Transcription factors such as AP1, ATF2, and c-Jun are compensated-activated when ERα activity is impaired, sustaining gene transactivation while activating intracellular signaling pathways including Ras/Raf/MEK/ERK1/2 and the PI3K/AKT [25, 26]. However, it is unclear what the molecular mechanism modulates ERα-mediated enhancer activation.

As one of the most important determinants of chromatin structure, CCCTC-binding factor (CTCF) participates in transcription processes, including enhancer-promoter looping and insulation [17, 27]. Studies have shown that CTCF is a critical protein that maintains and participates in ERα-mediated enhancer and promoter transactivation [28, 29]. The existence

¹Department of Cell Biology, Key Laboratory of Medical Cell Biology, Ministry of Education, School of Life Sciences, China Medical University, Shenyang City 110122 Liaoning Province, China. ²Department of Breast Surgery, Cancer Hospital of China Medical University, Liaoning Cancer Hospital & Institute, Shenyang City 110042 Liaoning Province, China. ✉email: yzhao30@cmu.edu.cn

Received: 15 July 2022 Revised: 9 February 2023 Accepted: 14 February 2023

Published online: 24 February 2023

of an ER α binding site (EBS) coupled with a CTCF binding site (CBS) provides the highest predictor score for estrogen-responsive genes [30, 31]. In breast cancer cells, CTCF binding is crucial not only for designing accessibility borders and insulated transcriptional blocks, but for modulating ER α -mediated gene expression [29, 30]. Also, CTCF modulates ER α -related genes by constructing higher-order chromatin structures for enhancer and promoter interactions with other proteins such as cohesin, ER α , or the transcription activators such as BRG1 [24, 32]. Furthermore, mutant ER α proteins could retain sustained transcription of downstream genes by binding FOXA1 and CTCF, suggesting that CTCF is able to reverse the loss of ER α -mediated transcriptional activity [33]. Even though CTCF plays a crucial role in enhancer function, the fundamental molecular mechanisms by which the two transcription factors interact on enhancers are unknown. Therefore, underlying a novel protein that administers this essential process is necessary.

Bromodomain PHD-Finger Transcription Factor (BPTF) associated protein of 18 kDa (BAP18) is encoded by C17orf49 gene in human. BAP18 is an 18 kDa protein that carries a SANT domain, which usually occurs in chromatin associated proteins such as Ada2, Swi3 and Rsc8 [34–36]. It is interesting to note that the SANT domain is more widely represented among enzymes that remodel chromatin than bromodomains or chromodomains, which suggests that BAP18 may play an important role in regulating chromatin accessibility. Researchers suggested that pulldown of BAP18 protein specifically copurified subunits of the human nucleosome remodeling factor (NuRF)/BPTF complex [37]. Several studies have shown that BAP18 is involved in nuclear receptors (NRs) mediated transactivation, including androgen receptor (AR) and ER α . Furthermore, BAP18 is highly expressed in a wide variety of cancers and diseases, including prostate cancer, ER α -positive breast cancer, oral squamous cell carcinoma, non-small-cell lung carcinoma, triple-negative breast cancer, and polycystic ovary syndrome (PCOS) [38–43]. It was previously reported that BAP18 significantly increases ER α -mediated transactivation in breast cancer, but the function of BAP18 on the enhancer region remains to be determined [40]. Using ChIP sequencing (ChIP-seq) analysis, we demonstrate that BAP18 recruits upon gene enhancer regions along with CTCF. BAP18 increases genome-wide accessibility of chromatin, particularly around CTCF recruiting sites. ER α -related enhancer transactivation is positively correlated with BAP18 enrichment density. A subunit of the nucleosome remodeling factor (NuRF) complex, BAP18 interacts with the necessary ATPases SMARCA1 and BPTF, and increases CTCF and ER α recruitment at enhancer regions. As a result, BAP18/CTCF facilitate enhancer-promoter looping of *TFF1* and *GREB1* in an estrogen-independent manner. BAP18 proliferates cell growth under the aromatase inhibitor and the enhancer inhibitors in MCF7 cells, and BAP18 is highly expressed in letrozole non-responders in clinical samples. Taken together, these data suggest a potential mechanism of ontogenetic enhancer activated by BAP18 and CTCF, and BAP18 might be an effective predictor of endocrine resistance.

MATERIALS AND METHODS

Cell lines and cell culture

In this study, breast cancer cell lines were obtained from the ATCC cell bank. T47D cells were cultured in an RPMI-1640 medium (Gibco) and MCF7 cells were cultured in a DMEM medium (Thermo Scientific). All cells were cultured with 10% fetal bovine serum (Gibco), 50 units/ml penicillin, and 50 units/ml streptomycin at 37 °C and 5% CO₂. 17 β -estradiol (E2, Sigma-Aldrich), Letrozole (MCE, HY-14248), JQ-1 (MCE, HY-13030), and THZ-1 (MCE, HY-80013) were dissolved in ethanol (Aladdin). The cells were cultured in phenol red-free DMEM or RPMI-1640 when drugs were needed. Culture dishes were purchased from Guangzhou Jet Bio-Filtration Co., Ltd., China.

Plasmids and antibodies

BAP18 overexpression plasmids were introduced in our previous work [38]. Two kinds of TFF1 core enhancers were respectively cloned into pGL3-promoter plasmids, and minimum promoter was cloned into the pGL3-enhancer plasmid to perform luciferase reporter assays. The primers for constructing inserted sequences of these regions were described in Supplementary Table 1.

The antibodies were used in our study as follow: anti-BAP18 (Bethyl #A304-207A-1), anti-ER α (Cell signaling #D8H8), anti-TFF1 (Proteintech 13734-1-AP), anti-SMARCA1 (Proteintech #29461-1-AP), anti-CTCF (CST #D31H2), anti-BPTF (Bethyl # A300-973A), anti- β -actin (Proteintech #20536-1-AP), anti-Rabbit/Mouse (ABclonal), anti-IgG (Proteintech#10238-1-AP), anti-GFP (Sigma #G1544) and anti-FLAG (Proteintech#20543-1-AP).

siRNA and CRISPR-Cas9 system

siRNA against BAP18, CTCF, and ER α were listed in Supplementary Table 2. All siRNA duplexes were purchased from Sigma-Aldrich.

Briefly, gRNAs were designed with tools on Zhang Feng's website (<http://CRISPR.mit.edu>), and construction procedures were followed by Zhang's study [44]. All gRNA sequences were listed in Supplementary Table 3. CRISPR-Cas9 plasmids were used in this study with Cas9-TFF1e-1, Cas9-SMARCA1-2, and Cas-BAP18-1, respectively.

Luciferase reporter assays

For a series of luciferase reporter assays, HEK-293 and MCF7 cells were co-transfected with BAP18 (200 ng), CTCF (75 ng), different pGL3 plasmids (200 ng), and a plasmid of control Renilla luciferase (pRL) (5 ng). Cells were cultured into a medium containing 5% charcoal-stripped fetal bovine serum after co-transfection for 4 h. After an additional day, cells were collected for luciferase reporter assay (Promega) after estrogen stimulation for 1 h. The final relative activity was calculated as the ratio of luciferase fluorescence value to pRL fluorescence value.

Western blotting and co-immunoprecipitation (co-IP) analysis

Western blotting assays were carried out using the usual procedure described in our prior work [45]. The immunoprecipitation analysis began with 2 h of whole-cell lysis purified with anti-IgG. If DNase (TAKARA#2270A) treatment was required after pre-clear, add 50 units of DNase/test to the experimental sample and incubate for 30 min at 37 °C. Protein G beads from GE Healthcare were condensed into sepharose and utilized for antibody-protein interactions, which were rotated overnight. Western blotting assays were performed after repeated three times rinses and lysis boiling.

RNA and quantitative real-time PCR (qPCR)

RNA Trizol (TAKARA) was used to extract total RNA, and cDNAs were reversed using the PimeScript RT-PCR kit (TAKARA). On the LightCycler 96, real-time qPCR experiments were carried out using the SYBR premeraseTaq kit (TAKARA) (Roche). All qPCR primers were described in Supplementary Table 4, and PRISM Graphpad 8 was used for statistics. Student *t*-tests were used to compare the results of each experiment, which were drawn from at least three separate trials.

Chromatin immunoprecipitation (ChIP) assays

We performed ChIP assays using Nature Methods standard protocols [46]. MCF7 cells were transfected with CRISPR-Cas9 system to knock out BAP18. The cells were cultured in phenol-free DMEM. The cells were treated with 100 nM E2 or equivalent EtOH for 1 h after they had reached 80% confluence. Following the studies, the DNAs were utilized as qPCR templates, and the primers were presented in Supplementary Table 5. The results were expressed as a percentage of input chromatin, and they are representative of at least three independent experiments. Using the *t*-tests, the significances of the difference between the two groups were determined.

MNase assays

All experiments were carried out in three biological duplicates. In MNase cleavage buffer (4 mM MgCl₂, 5 mM KCl, 50 mM Tris-HCl (pH 7.4), 1 mM CaCl₂, 12.5% glycerol), nuclei were digested under either Light MNase conditions (40 gel units for 15 min at 37 °C) or Heavy MNase conditions (40 gel units for 30 min, then another 40 gel units for 30 to 40 min at 37 °C) with 50 mM EDTA, and the MNase digestion processes were halted. The

protein-DNA crosslinks were then reversed by incubating the MNase-digested nuclei overnight at 60 °C with 0.2 mg/mL proteinase K and 1% sodium dodecyl sulfate. The samples were then run, and the nucleosome ladder was separated on a 2% agarose gel. Details were followed by standard protocol [47].

Chromosome conformation capture qPCR (3C-qPCR) analysis

3C-qPCR was performed following standard protocols [48]. In details, 1×10^6 MCF7 cells were harvested in PBS for each 3C sample. The cells were centrifuged at 300 *g* for 5 min at room temperature and resuspended in PBS with 10% FBS (final). For crosslinks, MCF7 cells were incubated with equal volume of 4% formaldehyde for 15 min and quenched with 2.5 M glycine solution, followed by centrifugation at 300 *g*/5 min/4 °C. Cell pellet was then resuspended in PBS/10%FBS and centrifuges at 300 *g*/5 min/4 °C. We discarded the supernatant and snapped-frozen it at 80 °C, and stored it at this temperature for a period of time. During 1.5 h at 4 °C, the cell pellet was lysed in lysis buffer (50 mM Tris-HCl pH 7.5, 0.5% NP-40, 1% Triton X-100, 150 mM NaCl, 5 mM EDTA, protease inhibitor cocktail (Roche)). Cell pellet was washed once in 1.2×restriction buffer and resuspended again in 500 µl of 1.2× restriction buffer. We added 15 µl of 10% SDS to suspension and incubated the mixture at 37 °C and shaking at 400 rpm. 75 µl of 20% Triton X-100 was added to the suspension and incubated at 37 °C and shaking at 400 rpm. Then the samples were centrifuged at 1000 *g* for 3 min and resuspended in 500 µl of 1×restriction buffer. Nuclei were pelleted and digested with the *Bgl* I restriction enzyme (NEB) for TFF1 transcriptome or *Hind* III for GREB1 at 37 °C overnight. An agarose gel was used the following day to assess digestion efficiency. Afterwards, the enzyme was inactivated at 65 °C for 20 min, and samples were centrifuged at 1000 *g* for three minutes to remove the restriction buffer. The pellet was resuspended in 7 mL of 1× ligation buffer, and the ligation was performed with addition of 50 U of T4 DNA ligase (5 U/µl) (Thermo Scientific) at 16 °C overnight. An agarose gel was used to test the ligation efficiency once again. The de-crosslinking process was carried out by adding 30 µl of protease K (Roche) to the sample overnight at 65 °C. The samples were incubated at 37 °C for 45 min with 15 mL of RNaseA cocktail (Ambion) in order to remove residual RNA. Using 7 mL of isopropanol and 70 mL of NucleoMag® P-Beads (Bioke), DNA was recovered by incubating the samples for 30 min at room temperature. The samples were then centrifuged for 3 min at 1000 *g* and washed twice with 80% ethanol. The beads were dried and eluted in 300 mL of 10 mM Tris-HCl pH 7.5. The purpose of 3C analysis was to assess the physical interactions between Enhancer^{TFF1}/Enhancer^{GREB1} and target regions. We designed a constant promoter primer (P) for each gene that amplifies the Enhance^{TFF1} or Enhancer^{GREB1} region overlapping the junction created by the *Bgl* I/ *Hind* III enzyme. To examine the interactions between Enhancer^{TFF1} or Enhancer^{GREB1} and each assessed region, we designed two primers (reverse and forward). 3C primers were listed in Supplementary Table 6. qPCR products were resolved on 2% agarose gel and also on quantitative PCR (qPCR). For the final 3C-qPCR assays, TFF1-R2 was used for the reverse primer of TFF1-related 3C-qPCR and GREB1-R1 for GREB1-related 3C-qPCR.

ChIP sequencing (ChIP-seq), ATAC sequencing (ATAC-seq) and data acquisition

MCF7 cells were treated with 100 nM E2 for 1 h after cell collection. MCF7 cells were contained in a 9 ml DMEM medium fixed with 243 µl 37% paraformaldehyde (Electron Microscopy Sciences, 15714) and crosslinked for 15 min at room temperature for two types of sequencing. The crosslinks were then broken down with 2.5 M glycine to a final concentration of 0.125 M. Cells were washed with cold PBS before tests were carried out with the assistance of Wuhan Seqhealth Tech Co. LTD. The primary analysis of ChIP-seq had been described, and the analysis of ATAC-seq was similar to ChIP-seq [40].

In this study, the GEO data series for ATAC-seq and ChIP-seq was GSE198243 (the access link of GSE198243). All other high-throughput data were obtained from other GEO datasets: GRO-seq data was from GSE73957, ATAC-seq data of estrogen stimulation in MCF7 was from GSE144925, ERα ChIP-seq data, and CTCF ChIP-seq data were from GSE108787, H3K27Ac data was from GSE40129, H3K4me1, H3K4me3, and RNA POL2 ChIP-seq data were from GSE23701, FOXA1 was from GSE161767. RNA-seq of clinical patients was from GSE145325 (PMID:29581135).

Cell growth assays, IC50 assays, and colony formation assays

All breast cancer cells were cultured for specific amounts of time before being harvested with trypan blue and counted with a hemacytometer. Single-cell suspensions were carried out with 1000 cells per 35 mm plate,

and cell growth line studies were carried out with 20000 cells per column. Cells were treated with various drug doses for 14 days for colony formation assays. Also, cells were treated with different concentrations of drugs for eight weeks, and cell counts were performed simultaneously to complete the IC50 assay.

Clinical patients and immunohistochemistry (IHC)

All primary breast cancer tissues and adjacent tissues of patients were procured from the Liaoning Cancer Hospital of China Medical University, all of which received permission from patients already. Under the guidance of a pathologist, all patients received immunohistochemistry to evaluate ERα, PR, HER2, and Ki67 expression by pathological puncture of tumor tissue. Patients who had been identified with ERα-positive but HER2-negative were given 12 weeks of neoadjuvant endocrine treatment with letrozole. After 12 weeks, post-treatment pathological puncture was used to evaluate ERα and Ki67 expression in tumor tissue. At the time of surgery, tumor sizes and lymph node metastases were measured. The widely recognized PEPI score was used to assess patient scores: a PEPI ≥ 4 was termed a letrozole non-responder, and a PEPI < 4 was regarded as a responder [49].

The procedure of IHC has been indicated in our previous work. The relative score of BAP18 expression was calculated as follows: Three fields of view were randomly selected for each specimen, ensuring that at least two or more typical breast ducts were included in the field of view. BAP18 staining of the ductal glandular luminal cells was calculated, and the grayscale values of the staining were tallied from brown (highest expression) to blue (lowest expression). Dark brown is defined as 0.03 points, light brown as 0.02, and blue as 0.01. Finally, the number of cells was multiplied by their respective coefficients as the final relative score.

Data analysis

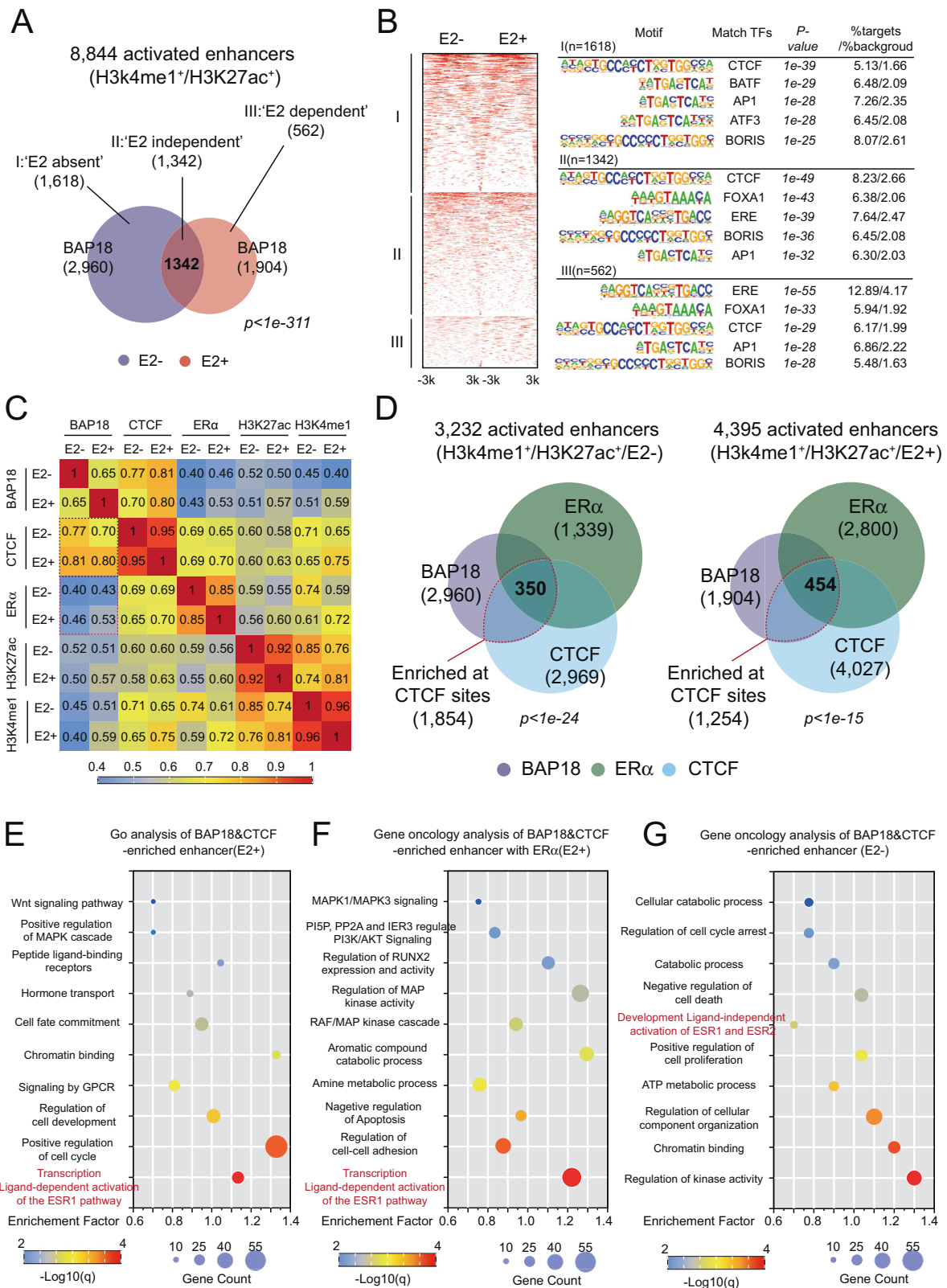
Column, Pie, Venn, Scatter, Violin boxes, and Line charts were performed using Prism GraphPad8 software. Heat and volcano plots were generated using OriginLab. Protein interaction predictions were predicted using the STRING website (<http://cn.string-db.org/>). GO analysis and GO_DisGeNET analysis were developed at the METASCAPE website (<http://metascape.org/gp/index.html#/main/step1>). The rest of the graphs were generated using R software.

For ChIP-seq and ATAC-seq data, the genomic location of the BAP18 peak can be classified using the R packages. The activated enhancers were defined by two histone modifications, H3K4me1 and H3K27ac, simultaneously merged. Defined enhancers containing EN numbers were compared to chromatin positions by downloading data from the Enhancer DB (<http://lcbw.swjtu.edu.cn/EnhancerDB/>). Correlation analysis method: ChIP-seq peak within the same locus (200 bp) was defined as X and formed a scatter plot with GRO-seq peak or ATAC-seq peak defined as Y value, and then correlation analysis was performed. In order to identify Peak on the genome, the ATAC-Seq Peak detection tool MACS2 was used to obtain the location of Peak on the genome, as well as the sequence information for Peak region. To scan the common motif between peaks, find the common motif region, and draw the motif map, Homer is used to extract the sequence of peak intervals. To analyze differences between groups, we used C_{sw} based on the edgeR framework.

RESULTS

BAP18 recruits on global enhancer regions with CTCF

It is well-recognized that estrogen and ERα induce massive transcriptional activation, accompanied by alterations in chromatin structure upon the global intergenic region containing gene enhancers. In our previous study, we revealed that a substantial quantity of BAP18 proteins recruited upon the intergenic regions, and the function of this part of BAP18 remains unknown. As a result, we identify the activation of the enhancer located in the intergenic region using enhancer hallmarks (ChIP-seq of H3K4me1 [50], H3K27ac [51] and GRO-seq [52], Fig. S1A). We identified 3232 activated enhancers without E2 (E2−) treatment and 4335 activated enhancers treated with E2 (E2+) in MCF7 cells (total: 8844 activated enhancers, Fig. S1B). Using the ChIP-seq data of BAP18, we identified 2960 BAP18-enriched activated enhancers in the E2− condition and 1904 BAP18-enriched activated enhancers in the E2+ condition (Fig. S1C, D). Among the 1342 activated enhancers with BAP18 recruitment, 1618 were E2-independent,



suggesting a potential role for BAP18 in modulating E2-independent enhancers (Fig. 1A). Then, we examined the possible transcription factor motifs on DNA among three different types of BAP18-enriched enhancers. It was found that the DNA motifs matched top-5 transcription factors such as CTCF, BATF, AP1,

ATF3, and BORIS in E2-absent groups. Conversely, the binding motif matched transcription factors such as CTCF, AP1, BORIS, ERα, and the pioneer factor FOXA1 in E2-independent and E2-dependent groups (Fig. 1B). To further investigate the characteristics of BAP18 in enhancer recruitment, we estimated the

Fig. 1 BAP18 recruits on global enhancer regions with CTCF. **A** A Venn diagram exhibited the overlap between ChIP-seq peaks for BAP18-enriched activated enhancers at a total 8844 enhancers, which were marked H3K4me1 and H3K27ac. *P*-value was calculated by hypergeometric tests. **B** As a result of motif analysis, the top 5 transcription factors associated with BAP18 were identified as follows: (I) E2-absent; (II) E2-independent; (III) E2-dependent. Heatmaps exhibited the signals ranging from -3 kb to +3 kb surrounding the center of each annotated BAP18 peak on enhancers. **C** Correlation analysis showed the correlation between the density of BAP18-enriched peaks on enhancers with CTCF, ER α , H3K4me1, and H3K27ac. The number represented the compared correlation score: the account of tags in the same region in two sequencing/the whole account of tags. **D** Venn diagrams were performed to determine whether ER α recruitment sites overlapped with BAP18 and CTCF co-recruitment sites with or without E2. Fisher's exact tests were performed. GO analysis demonstrated the functional pathways involved in the co-recruitment of enhancers by BAP18 and CTCF with estrogen treatment (**E**), or with estrogen treatment combined with ER α (**F**), or without estrogen treatment (**G**). The bubble color represented by Log₁₀(q), and the bubble size represented the number of genes in the relevant pathway. Enrichment factor = gene in GO/gene in hit list * 100%. *Q*-value is the multi-test adjusted *p*-value, presenting by metascape website (<http://metascape.org/>).

activated enhancers which CTCF and ER α were recruited (Fig. S1E–H). It is evident that there was a strong correlation between BAP18-enriched density and enhancer hallmarks. Also, BAP18-enriched enhancer peak density had a stronger correlation with CTCF (black box) than ER α (red box) enhancer enrichment density (Fig. 1C). These results indicated that CTCF was an important transcription factor involved in the enrichment of BAP18 at activated enhancers.

When BAP18 and CTCF were co-recruited to enhancers, we wondered how many of them had simultaneous ER α recruitment. The results showed that without estrogen treatment, only 18.88 percent of enhancers ($n = 350$) had contemporaneous recruitment of BAP18, CTCF, and ER α [17], whereas 36.2 percent of these ($n = 454$) had concomitant recruitment of BAP18, CTCF, and ER α with E2 (Fig. 1D). According to the results, only a small proportion of the enhancers co-recruited with BAP18 and CTCF are ER α -dependent. Gene ontology analysis revealed the biological functions of these enhancer-related genes. It was discovered that the enhancer-related genes recruited by BAP18 and CTCF when estrogen was administered were involved in gene functions, such as transcription ligand-dependent activation of the ESR1 pathway, positive regulation of cell cycle, regulation of cell development, signaling by GPCR, and cell fate commitment (Fig. 1E). Meanwhile, those enhancer-related genes recruited by BAP18 and CTCF in conjunction with ER α have been involved in not only transcription ligand-dependent activation of the ESR1 pathway but also in cell-cell adhesion regulation, negative regulation of apoptosis, RAF/MAP kinase cascade, and regulation of MAP kinase activity (Fig. 1F). Interestingly, gene functions included the development of ligand-independent activation of ESR1 and ESR2 signaling in the absence of estrogen treatment, of which BAP18 and CTCF-enriched enhancers, implying that BAP18 has ER α -independent recruitment on ER α -related enhancers with CTCF regardless of estrogen treatment (Fig. 1G). Based on the results of these studies, BAP18 might function in collaboration with CTCF at gene enhancers, not only include ER α -related enhancers.

BAP18 facilitates a widespread chromatin accessibility

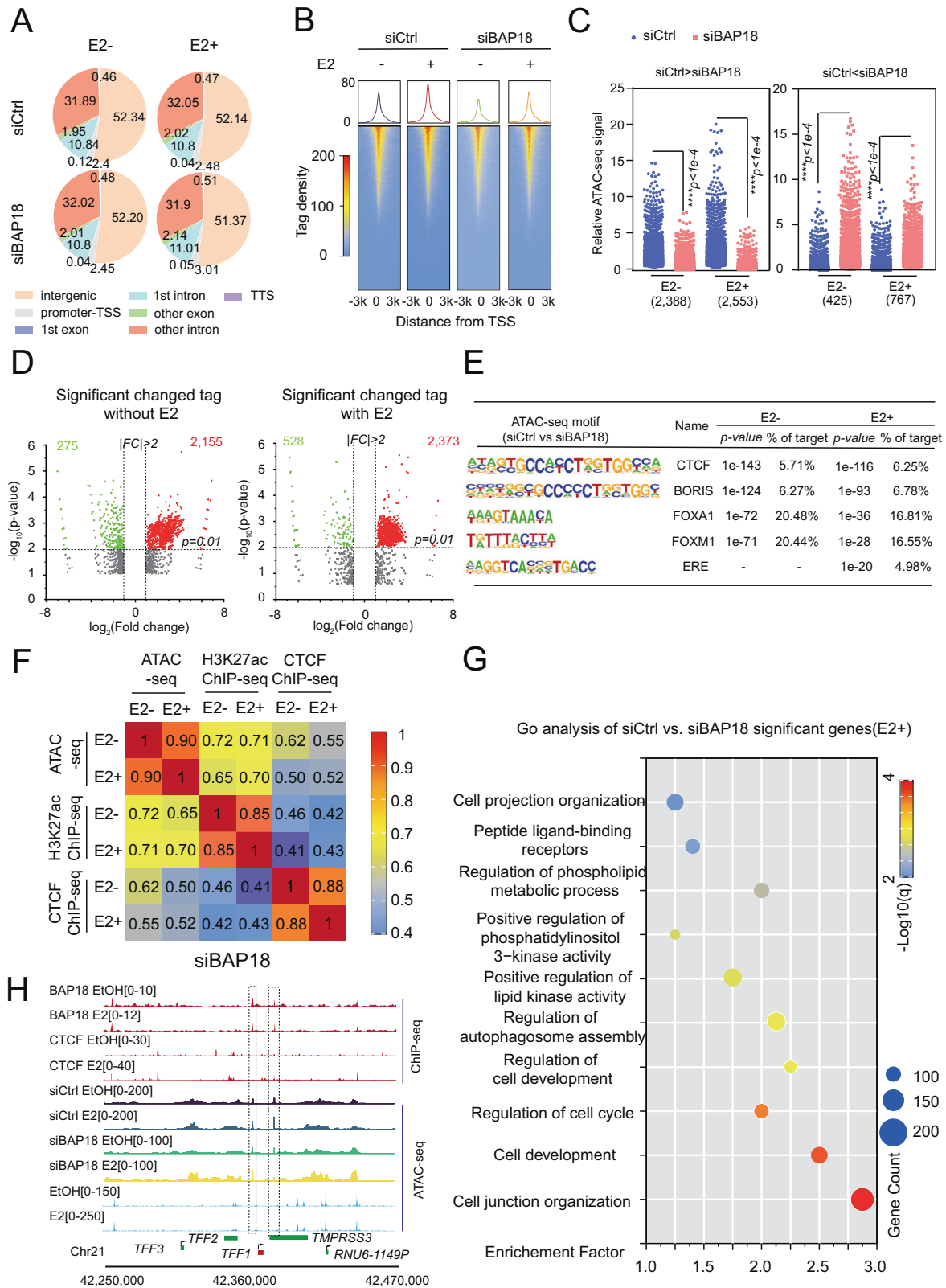
Since BAP18 contains a SANT domain, it is probably that chromatin remodeling occurs during the process of BAP18 recruitment to enhancer regions. In order to evaluate this potential function, ATAC-seq was performed in MCF7 cells to detect the chromatin accessibility with BAP18 silencing. Consistency with the random peaks control, more than half of these high confidence peaks were located in intergenic regions, suggesting that BAP18 had less impact on the genomic distribution of chromatin accessibility among all four groups (Figs. 2A and S2A). Importantly, the depletion of BAP18 significantly reduced the density of chromatin accessibility peaks throughout the genome (Fig. 2B). Among these changed peaks ($FC > 1.5$), we identified 2388 less accessible enhancers under silencing of BAP18 without E2 and 2553 enhancers under E2 treatment. By contrast, only 425 and 767 enhancers had increased chromatin accessibility under

BAP18 depletion (Fig. 2C). A great number of enhancers with reduced chromatin accessibility were observed under BAP18 depletion than enhancers with improved chromatin accessibility (Fig. 2D). The results indicated that BAP18 mainly affected the degree of site-specific accessibility across the genome. Then, DNA motif analysis was utilized to determine how BAP18 altered chromatin accessibility within genome-wide enhancer regions. It was not surprising that CTCF was the most closely matched transcription factor for the significant ATAC-seq peak on the enhancer, along with BORIS, FOXM1, ER α , and the pioneer factor FOXA1 (Fig. 2E). The results suggested that BAP18 might modulate the chromatin remodeling and consequent transcriptional activation in the enhancer regions with CTCF. ATAC-seq was compared to the H3K27ac modification and the CTCF ChIP-seq, and multiple connections were observed between the ATAC-seq intensity and enhancer hallmarks (Figs. 2F and S2B). Following the silencing of BAP18, we conducted a gene ontology analysis to determine which genes were significantly altered. Based on the results, the genes with the greatest chromatin accessibility changes were primarily involved in the cell cycle regulation, cell morphogenesis in differentiation, cell junction organization, and cell development (Figs. 2G and S2C). Additionally, we mapped the transcriptome genome browsers of the *TFF1* and *GREB1* genes, which occupied enhancers associated with CTCF and BAP18. The results showed that BAP18 strengthened the chromatin accessibility of promoter and enhancer regions, but silencing BAP18 decreased its chromatin accessibility, along with less CTCF enrichment (Figs. 2H and S2E). These data demonstrated that BAP18 significantly impacted genome-wide chromatin accessibility, particularly within CTCF-enriched enhancer regions.

MNase assays in ER α -positive breast cancer cells were used to investigate BAP18's influence on chromatin accessibility. MNase digestion increased the quantity of residual chromatin in the siBAP18 group, demonstrating that chromatin accessibility decreased as BAP18 expression decreased (Fig. S3A). Similar conclusions were found in T47D cells (Fig. S3B). Consistent with our previous findings, BAP18 modulated chromatin accessibility regardless of whether these cells were exposed to estrogen. Similarly, overexpression of BAP18 resulted in a substantial decrease in the amount of MNase digested chromatin remaining in MCF7 and T47D cells (Fig. S3C, D). Using the leftover DNA as a template, we performed qPCR assays to confirm these results. The qPCR results showed that the promoter and enhancer DNA templates of *TFF1*, *MYC*, and *GREB1* were enhanced when compared to the control group (Fig. S3E). Based on these results, BAP18 showed an ability to enhance chromatin accessibility of CTCF-enriched enhancers.

E2-induced enhancer activation is positively correlated with BAP18 recruitment

According to GRO-seq data, genome-wide transcriptional status was determined as well as whether response elements were active under estrogen. In MCF7 cells, we analyzed the relationship



between GRO-seq and the intensity of BAP18-enriched enhancer peaks in order to evaluate whether BAP18 enrichment is associated with enhancer transactivation. Regardless of estrogen treatment, BAP18 recruitment intensity was moderately correlated with the GRO transcriptional activation state of the same

enhancers ($r > 0.5$, Fig. 3A). Due to this, we examined the relationship between BAP18-enriched density and estrogen-induced gene transcription. Among all BAP18-enriched enhancers from ChIP-seq data (total=2723), 1608 active enhancers on which BAP18 recruitment increased in response to E2 (59.05%), while

Fig. 2 BAP18 facilitates a widespread increase in chromatin accessibility. **A** Pie charts showed the distribution of differential ATAC peaks on genome intensity between control and siBAP18 groups that were treated for 1 h with or without estrogen. **B** Tag density distribution indicated the intensity of chromatin accessibility and tag distance from TSS in 4 groups. **C** The histogram exhibited the number of enhancers with increased accessibility or decreased accessibility with or without E2 treatment under BAP18 depletion. *T*-tests were performed. **D** Volcano plots screening exhibited a significantly change among accessible enhancers. Fold enrichment change (FEC) was defined as the fold enrichment of genes treated with estrogen minus the fold enrichment of genes without estrogen treatment. $FEC < -2$ was represented the significant increased accessibility with siBAP18, whereas $FEC > 2$ was represented the reduced accessibility with siBAP18. Adjusted *p*-value < 0.01 . **E** Following the silencing of BAP18 in ATAC-seq, DNA motif analysis revealed relevant tag-matching transcription factors. **F** Correlation analysis showed the correlation between the density of ATAC-seq peaks on enhancer with CTCF enrichment or H3K27ac modification in the BAP18 silencing group. The number represented the compared correlation score: the account of tags in the same region in two sequencing/the whole account of tags. **G** Bubble diagrams indicated related signaling pathways of all significantly-changed genes in estrogen conditions. **H** Genomic browser snapshots showed BAP18 and CTCF enrichment in the presence or absence of estrogen (Red) and ATAC-seq peaks of four groups with estrogen-induced on the *TFF1* gene areas. The light blue peaks represent the E2-associated ATAC-seq data in MCF7 cells downloaded from the GEO database. Boxed regions denoted considered enhancer and promoter areas. The genomic locations and read counts are shown above.

1,115 decreased in response to E2 (40.95%, Fig. 3B). A GRO-seq analysis in MCF7 cells revealed that estrogen treatment resulted in 60% gene activation ($n = 1680$) and 40% gene repression ($n = 1120$). Based on changes in BAP18 recruitment on activated enhancers, we evaluated two columns of estrogen-induced genes and found that 60.77% of E2-activated genes had increased BAP18 recruitment, while 70.98% of E2-suppressed genes had decreased BAP18 recruitment (Fig. 3C). BAP18 recruitment was positively correlated with more than half of the changes in gene transcriptional status, suggesting that BAP18 recruitment at enhancers significantly modulate gene expression.

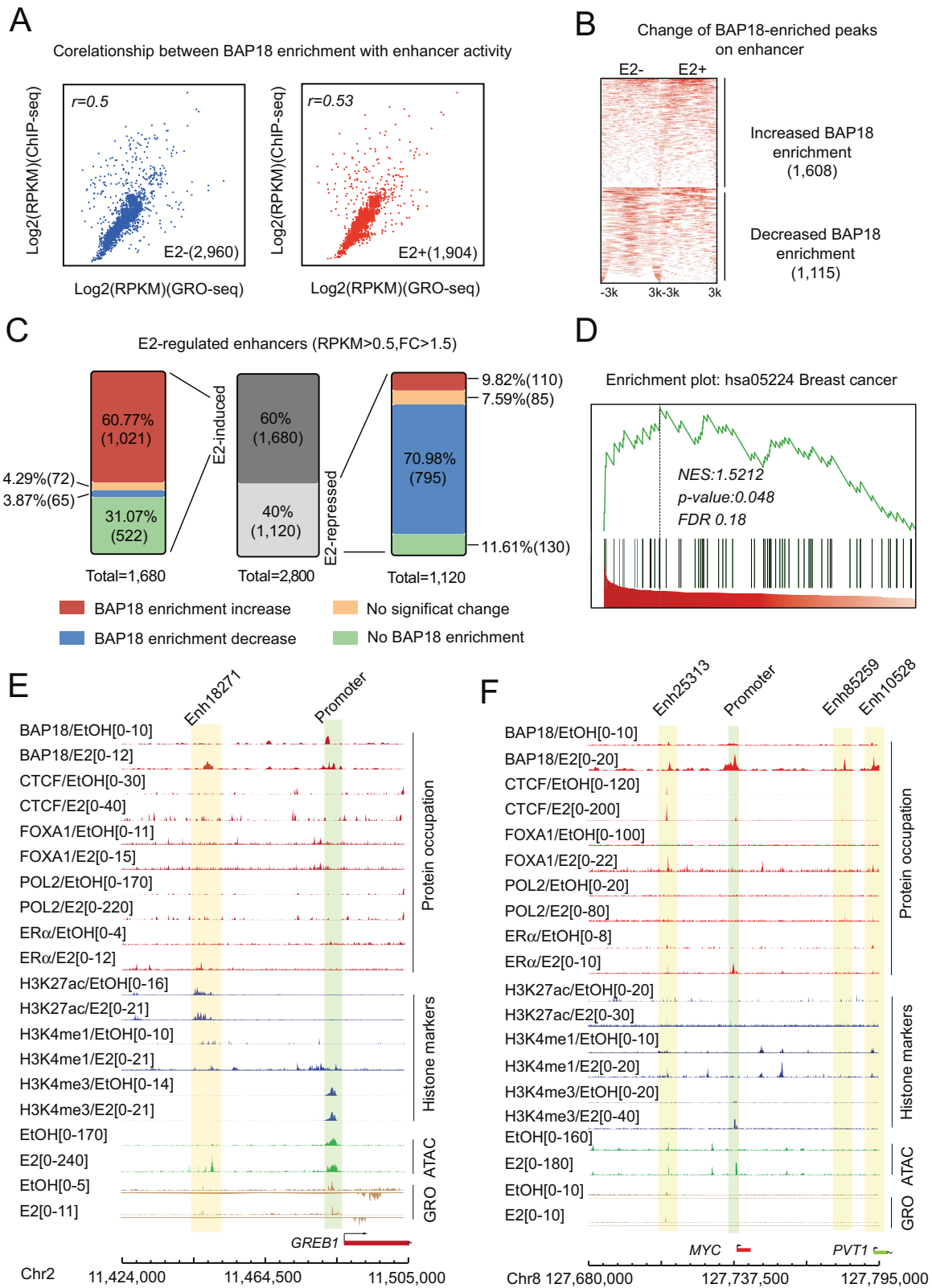
Then, we analyzed all genes with BAP18-enriched enhancers using a volcano plotting analysis ($|\text{Fold change}| > 2$, $p < 1e-3$). The findings revealed 688 E2-associated genes with increased BAP18 recruitment on enhancers such as *GREB1*, *TFF1*, *MYC*, and *NRIP1*. There were also 645 E2-associated genes with substantially decreased BAP18 enrichment, such as *ADGRV1*, *ZNF44*, *NPR3*, and *LMO3* (Fig. S4A). We found numerous typical E2/ER α target genes that were thought to promote breast cancer growth within the group of highly elevated genes (EtOH vs. E2). Analyzing these significantly altered genes by GESA analysis and the results showed that these genes can be significantly enriched in the breast cancer pathway (Fig. 3D). Surprisingly, there was a moderate BAP18 enrichment on the enhancers without E2 treatment (such as *TFF1* and *GREB1*), accompanied by adequate transcriptional activity, suggesting that BAP18 may affect the enhancer activity of these oncogenes in estrogen-free or estrogen-deprivation conditions. Additionally, we identified promoter and enhancer genomic browser diagrams using R software and the Enhancer DB database for *GREB1*, *MYC*, and *TFF1* (Figs. 3E, F, and S4B). In addition to increasing BAP18-enriched peaks, higher levels of the H3K27ac and H3K4me1 were observed on activated enhancers of these genes. Furthermore, increased BAP18 recruitment was associated with enhanced protein enrichment, including CTCF, POL2, and ER α . Statistical analysis of ATAC-seq and GRO-seq data indicated that BAP18-recruited enhancers exhibited increased transcriptional activity and chromatin accessibility. These findings suggested that enhanced BAP18 enrichment at enhancer regions correlated with E2/ER α -related enhancers activation and may be implicated in activating these oncogenes.

BAP18 associates with NuRF complex to promote CTCF recruitment on activated enhancers

Using siRNAs targeting BAP18, CTCF, and ER α , we discovered that silencing BAP18, CTCF, and ER α in MCF7 cells did not affect each other's RNA or protein expression (Fig. S4C, D). Following that, ChIP assays were performed to detect the recruitment of BAP18, CTCF, and ER α to the enhancer regions of traditional E2/ER α -related genes, including *GREB1*, *TFF1*, *MYC*, *CCND1*, *E2F1*. The findings revealed a distinct increase of BAP18 recruitment

upon various gene enhancers under estrogenic conditions, accompanied by enhanced recruitment of CTCF and ER α (Fig. 4A). Considering BAP18 is a subunit of the chromatin remodeling complex NuRF, we speculated that BAP18 facilitated transcription factor enrichment on chromatin together with the remodeling enzymes in NuRF. SMARCA1 and BPTF have been identified as critical remodeling enzymes of NuRF to modulate chromatin accessibility. Using the STRING database, we discovered a possible interaction among BAP18, SMARCA1, BPTF, and CTCF (Fig. S4E). Endogenous co-IP assays revealed that BAP18 interacted with SMARCA1, BPTF, CTCF, and ER α with E2 treatment. DNase treatment attenuates the interaction between BAP18 and these proteins, suggesting that our protein complexes are dependent on chromatin/DNA (Fig. 4B). When SMARCA1 was knocked out by CRISPR-Cas9 system, the interaction between BAP18 and two transcription factors was not significantly changed, and DNase might partially attenuate this interaction, suggesting that SMARCA1 does not play a dominant role in BAP18-CTCF/ER α interactions (Fig. 4C). The knockout of BAP18 resulted in significantly weakened interaction among the complex subunits, indicating that BAP18 plays a crucial role in the interplay between proteins (Fig. 4D). In MCF7 cells, siRNAs against ER α or CTCF were used to determine if the connection between SMARCA1 and BAP18 relied on the two transcription factor proteins (Fig. S5A). The results showed that the interaction between BAP18 and SMARCA1 significantly changed after silencing CTCF but not ER α , indicating that CTCF also played an essential role in the interaction of BAP18 with NURF complex proteins, as well as BAP18 had more involvement in CTCF-mediated DNA binding through the NURF complex. As a contrast, the BAP18-SMARCA1 interaction exhibited limited influence within ER α , suggesting that the ER α is not dominant in the overall transcriptional module recruitment and interaction process. A GFP-tagged BAP18 truncated mutation plasmids were transfected into MCF7 cells to further detect the protein interaction regions. It was found that SMARCA1 interacted with both the full-length and N-terminal truncated BAP18 plasmids, but not with the C-terminal truncated plasmid. Similar to our previous findings, CTCF and ER α primarily interacted with the full-length and N-terminal regions of BAP18 and only weakly with the C-terminal region (Figs. S5B, C). Given that the N-terminal of BAP18 contains a SANT domain that acted DNA or chromatin interaction function, these findings suggested that BAP18 was the essential protein influencing the interaction of BAP18/SMARCA1/BPTF/CTCF or ER α protein complexes, which was partially chromatin dependent.

The results of these ChIP assays were analyzed for the enrichment of BAP18, SMARCA1, CTCF, or ER α protein complexes at the transcriptional region (including CTCF binding site (CBS) or ER α binding site (EBS)) of *GREB1*, *TFF1*, and *MYC*. The After knocking out BAP18, both SMARCA1 and CTCF



recruitment in the CBS regions were reduced differentially (Fig. 4E). By contrast, SMARCA1 knockout did not affect the recruitment of BAP18 and CTCF in the CBS regions (Fig. 4F). Similar results were discovered on the EBS of the three genes

(Fig. S5D and E). All of the above findings suggested that BAP18 played an essential role in modulating transcription factors recruitment and may be required for NURF to regulate gene enhancer transactivation.

Fig. 3 E2/ER α -induced enhancer activation positively correlates with increased BAP18 recruitment. **A** Scatter plot analysis represented the relationship between BAP18 tag intensity at the enhancer and transcriptional intensity in the same area under estrogen-free and estrogen-treated conditions. **B** The heat map indicated the two types of enhancers: increased enrichment or decreased enrichment of BAP18 tag intensity. **C** Parts of whole diagrams showed the proportion of enhancer activity regulated by estrogen. 60% ($n = 1680$) of all E2-altered transcriptional state peaks were induced to activate by E2, whereas 40% ($n = 1,120$) were repressed by E2. **D** GESA plots exhibited the breast cancer-hallmarks signature with the BAP18-enriched E2-induced gene data. NES represents the normalized Enrichment score (ES = The degree of enrichment at the top or bottom of this sequence after sorting of all hybridized data). FDR determines the rate of false positives that may be included, and $FDR < 0.25$ is allowed. The p-value describes the statistical significance of the enrichment score obtained for a subset of functional gene. **E** Following estrogen treatment, a volcano plot analysis identified substantial BAP18-binding genes on enhancer regions. Fold enrichment change (FC) was defined as the fold enrichment of genes subjected to estrogen therapy minus those subjected to no treatment. Green plots represented $FEC < -2$, whereas red plots represented $FEC > 2$. Genomic browser snapshots indicated several kinds of enhancer features upon *GREB1* (**E**) and *MYC* (**F**) transcriptome. Protein occupation included BAP18, CTCF, FOXA1, POL2, and ER α enrichment in the presence or absence of estrogen (Red). Several histone modifications included H3K27ac, H3K4me1, and H3K4me3 (Blue). Chromatin accessibility is indicated using ATAC-seq (green), and real-time genomic transcription is indicated using GRO-seq (brown). Box contents represented known promoter and potential enhancer regions of candidate genes. Genomic coordinates and read counts are indicated above.

BAP18/CTCF enhances the transcriptional activity of TFF1 enhancers

Following our initial detection of eRNA and mRNA expression of E2-associated enhancers, we examined how the recruitment of BAP18 controls transcriptional activity of E2 enhancers. BAP18 depletion significantly decreased the eRNA expression of *GREB1*, *TFF1*, *MYC*, *CCND1*, and *E2F1*, whereas silencing CTCF significantly decreased four other eRNA genes in addition to *E2F1* (Fig. 5A, B). Also, depletion of both BAP18 and CTCF resulted in a significant reduction in mRNA expression. We then explored transcriptional activity of TFF1 using luciferase assays. pGL3 plasmids containing the TFF1 enhancer and promoter were constructed, and both of these truncated plasmids have CTCF and ER α binding sites. In addition, we designed simple enhancers containing the CTCF binding site (Fig. 5C). The luciferase assays results showed that BAP18 significantly enhanced the transcriptional activity of the TFF1 promoter throughout CTCF overexpression. Interestingly, BAP18 enhanced the transcriptional activity without estrogen, demonstrating that BAP18 might promote TFF1 expression with CTCF expression without estrogen in both MCF7 cells and HEK293 cells (Figs. 5D and S6A). By using siRNA against CTCF, significant reductions in TFF1 enhancer activity were observed without estrogen, suggesting that BAP18 may partially control TFF1 enhancer activity via CTCF (Fig. 5E). Furthermore, after knocking out SMARCA1, transcriptional activation of the TFF1 enhancer by BAP18 was reduced, but transcriptional activity still increased, suggesting that BAP18 plays an essential role in regulating TFF1 enhancer activity by controlling NuRF subunits participating in transcription (Fig. 5F). Based on these findings, BAP18 increased TFF1 eRNA expression with CTCF in an estrogen-independent manner, activating TFF1 enhancer activity.

BAP18 facilitates enhancer-promoter looping of ER α -regulated genes

Following these conclusions, we sought to gain a deeper mechanistic understanding of the molecular mechanisms underlying the E2-related transcriptome and epigenome. Due to the fact that the eRNA and mRNA of these E2-related genes are regulated simultaneously, a physical interaction between the promoters of these genes and the BAP18/NuRF/CTCF-bound enhancers should be expected. We combined the ChIP-seq and ATAC-seq of BAP18 to create Chromosome Conformation Capture quantitative PCR (3C-qPCR) system (Fig. 6A). After silencing BAP18, the signaling between the potential Enhancer^{TFF1}-U11 site (enhancer of TFF1-upstream No.11 site) and the Promoter^{TFF1} (promoter of TFF1) was drastically decreased. BAP18 silencing also significantly decreased the looping signal between the Enhancer^{TFF1}-D1 site and the Promoter^{TFF1}. Furthermore, depletion of BAP18 might reduce the strength of looping signals in the absence of estrogen, demonstrating that BAP18 could control TFF1 enhancer-

promoter looping in an estrogen-independent manner (Fig. 6B, C). siRNA against CTCF was utilized to examine the extent to which CTCF influences enhancer-promoter looping. Indeed, the data demonstrated that silencing CTCF reduced the enhancer-promoter looping signal at the Enhancer^{TFF1}-U11 site and Enhancer^{TFF1}-D1 site, and overexpression of BAP18 rescued the looping connections (Fig. 6D, E).

Similarly, *GREB1* enhancers were all found upstream of the promoter, and we discovered putative enhancers in the Enhancer^{GREB1}-U3 to Enhancer^{GREB1}-U2 loci (Fig. 6F). 3C-qPCR analysis revealed that silencing BAP18 inhibited the development of enhancer-promoter looping at both the Enhancer^{GREB1}-U3 and Enhancer^{GREB1}-U2 sites. The increased looping signal at the Enhancer^{GREB1}-U3 locus was more apparent than at the Enhancer^{GREB1}-U2 locus, most likely because BAP18 was recruited more at the Enhancer^{GREB1}-U3 site (Fig. 6G, H). Conversely, reducing CTCF lowered looping levels at the Enhancer^{GREB1}-U3 and Enhancer^{GREB1}-U2 sites, which was completely reversed by BAP18 overexpression (Fig. 6I, J). All of the above findings indicated that BAP18/CTCF complex mediated TFF1 and GREB1 activation via enhancer-promoter loops.

BAP18 depletion conferred the sensitivity to aromatase inhibitors or enhancer inhibitors

Clinically, aromatase inhibitors are used as the first-line treatment for ER+ breast cancer patients, which attempt to prevent estrogen synthesis and inhibit the transcriptional activity of E2/ER α -related genes. In light of the remarkable impact of BAP18 on transcriptional regulation in the absence of estrogen, we were interested in investigating its potential role in aromatase inhibitor therapy. Through an IC50 analysis, we determined that MCF7 cells are more sensitive to letrozole (the most-used AI drug, $IC_{50} = 5 \times 10^{-6}$ M) than T47D cells ($IC_{50} = 5 \times 10^{-5}$ M, Fig. S7A). As a result of using CRISPR-Cas9 system to knock out BAP18 (BAP18-KO) in MCF7 cells, we found that depletion of BAP18 significantly enhanced the sensitivity of MCF7 cells to letrozole (IC_{50} changed from 10^{-6} M to 10^{-7} M, Fig. 7A). The letrozole-resistant MCF7 cell line (MCF7-LetR) was established in 8 weeks, with the BAP18 knockout group of cells failing after the fourth week, indicating that BAP18 played an essential role during letrozole resistance process (Fig. 7B). After successfully constructing letrozole resistance cells, we carried out cell clone generation and growth assays (Fig. 7C). At same letrozole concentrations, BAP18 knockout significantly decreased survival in both MCF7 parental cells and MCF7-LetR cells (Fig. 7D). Similarly, after the temporary knockout of BAP18 in MCF7-LetR cells, previously letrozole-insensitive cells failed to survive, indicating that BAP18 might have a dramatic impact on the survival of MCF7 cells with letrozole treated (Fig. 7E). Given that TFF1 is crucial in breast cancer proliferation during endocrine treatment, we hypothesized that BAP18 depletion partially affected cell growth under letrozole through TFF1. We discovered

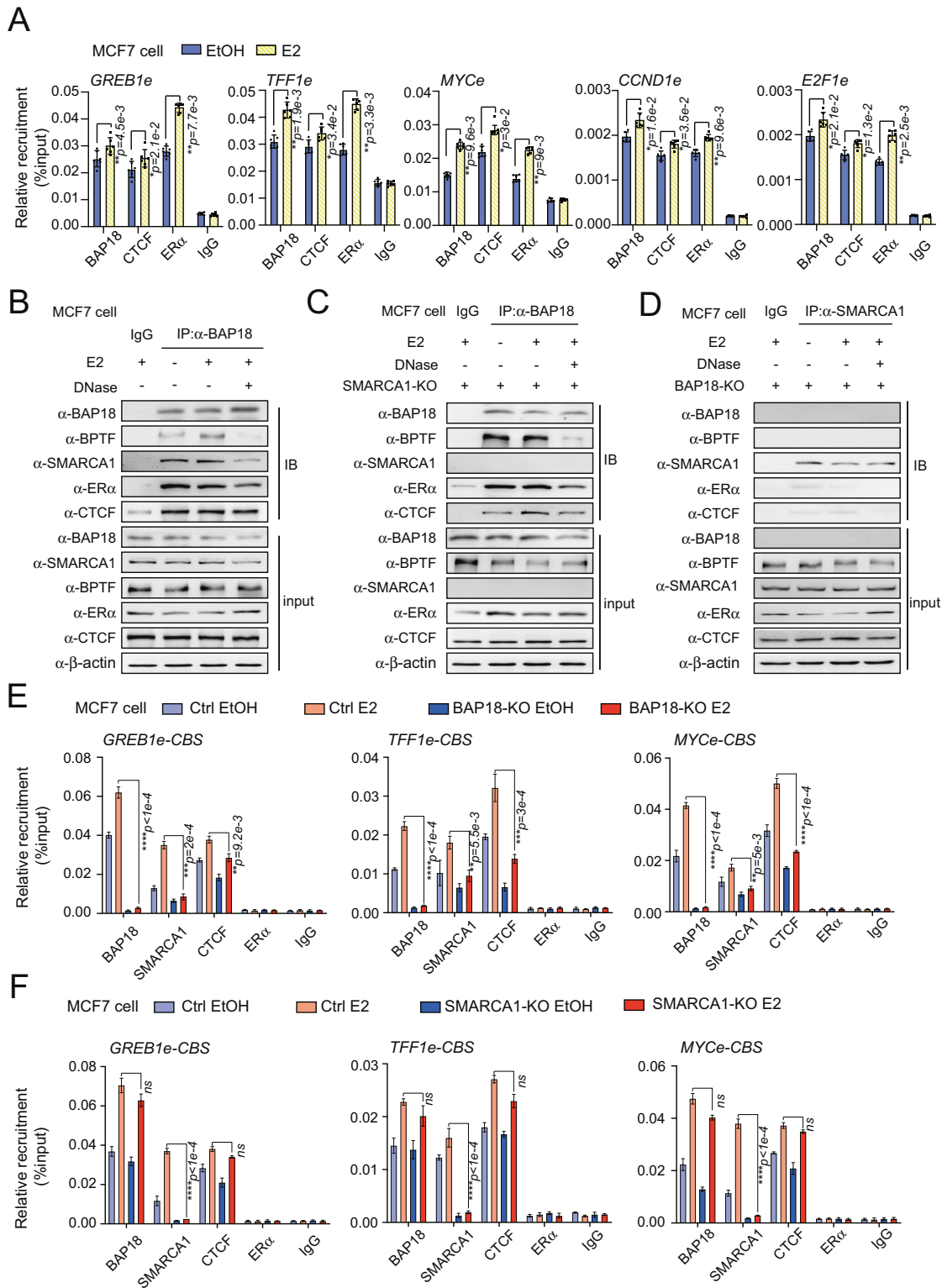
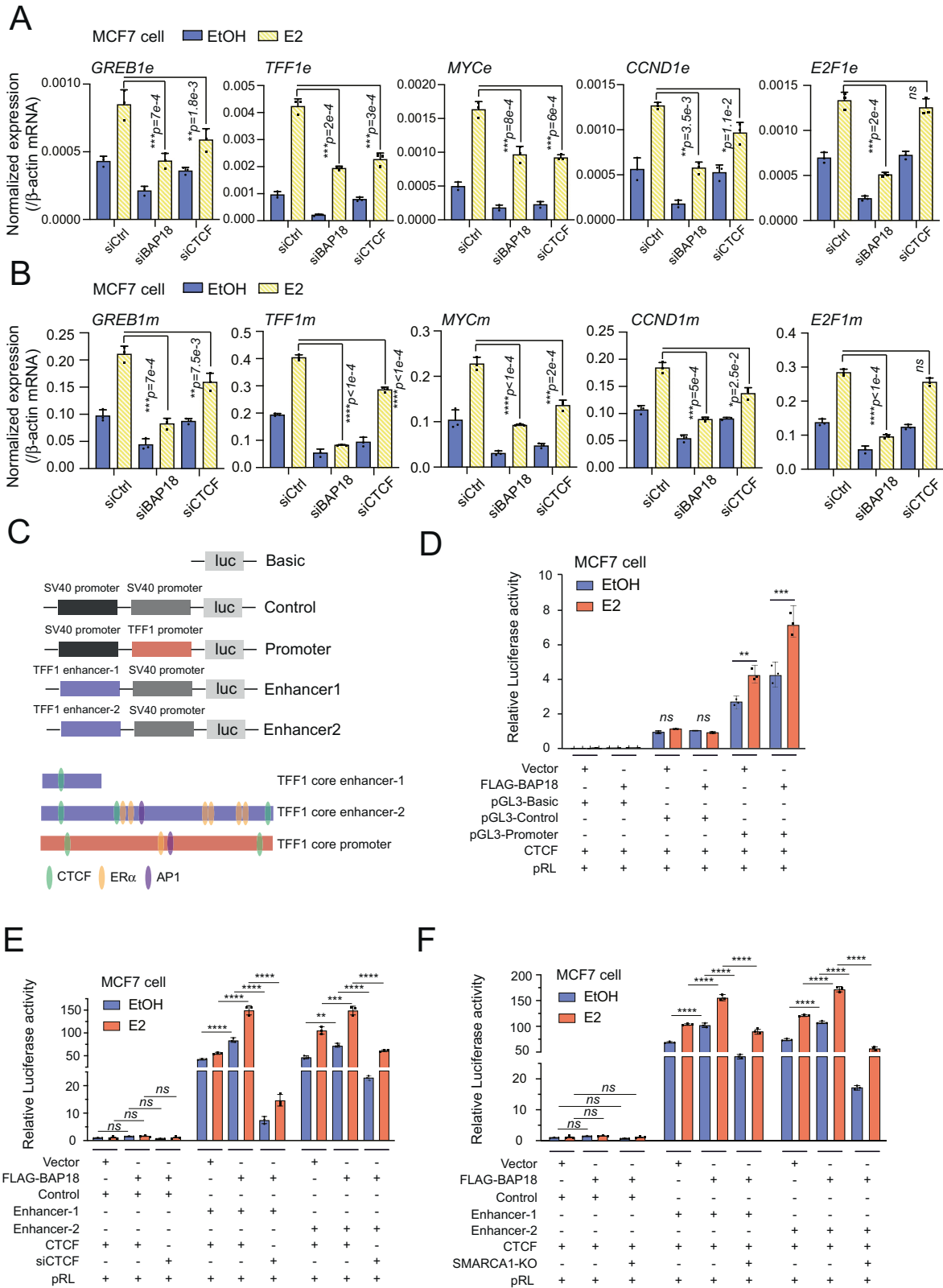


Fig. 4 BAP18 interacts with NuRF complex and promotes CTCF recruitment on E2-related enhancers. **A** ChIP q-PCR assays showed the recruitment of three proteins (including BAP18, CTCF, and ERα) in *GREB1*, *TFF1*, *MYC*, *CCND1*, and *E2F1* enhancer regions; blue bars represented equal EtOH treatment, yellow bars represented E2 treatment. The figure showed the results of at least one of the three independent experiments and *t*-tests were used. Co-IP experiments demonstrated the interaction between endogenous BAP18 with BPTF, SMARCA1, ERα, and CTCF in normal culture (**B**), or SMARCA1 knockout using CRISPR-Cas9 system (SMARCA1-KO (**C**)), or BAP18 knockout (BAP18-KO (**D**)). DNase was used to illustrate whether the interaction exists in DNA-free conditions. ChIP q-PCR experiments demonstrated the recruitment of BAP18, SMARCA1, CTCF, and ERα in BAP18-KO (**E**) or SMARCA1-KO (**F**) at the CTCF binding site (CBS) on the three gene enhancers. The statistical significance of all qPCR assays was determined using *t*-tests. Error bars represented mean \pm SD. * $p < 0.05$, ** $p < 0.01$, *** $p < 1e-3$, **** $p < 1e-4$ and *ns* represented no significant. At least one of the three independent experiments was represented.



that eRNA expression was unchanged for eight weeks following letrozole treatment except for *TFF1*, whereas eRNA expression for *GREB1*, *MYC*, and *CCND1* decreased (Fig. S7B). MCF7-LetR cells previously resistant to letrozole recovered the sensitivity after

CRISPR-Cas9 knockout of the enhancer regions of *TFF1*. This result indicated that the *TFF1* enhancer and its eRNA play a critical role in letrozole resistance (Fig. S7C). Furthermore, siRNA against to inhibit *TFF1* eRNA restored letrozole sensitivity in MCF7-LetR cells,

Fig. 5 BAP18 activates the transcriptional activity of TFF1 enhancers with CTCF. qPCR analysis was examined for demonstrating the eRNA (A) and mRNA (B) expression of estrogen-induced genes in MCF7 cells transfected with control siRNA (siCtrl) or siRNAs specific against BAP18 (siBAP18) and CTCF (siCTCF) under estrogen treatment. The statistical significance of all qPCR assays was determined using *t*-tests. Error bars represented mean \pm SD. * $p < 0.05$, ** $p < 0.01$, *** $p < 1e-3$, **** $p < 1e-4$ and *ns* represented no significant. Three independent experiments were performed. C The schematic diagram exhibited the pGL3 plasmid used for Luciferase assays. The enhancer and promoter of TFF1 contained potential binding sites for CTCF (green), AP1 (purple), and ER α (yellow). D BAP18 enhances CTCF-induced TFF1 promoter transactivation in MCF7 cells. The cells were co-transfected with overexpression plasmids of CTCF together with FLAG-tagged BAP18 expression plasmid (FLAG-BAP18) or PcDNA3.1 plasmids (Vector) with (red histograms) or without (blue histograms) E2 treatment (100 nM). Luciferase assays exhibited the function of CTCF protein (E) or SMARCA1 protein (F) in TFF1 enhancer transactivation. The statistical significance of all Luciferase assays was determined using *t*-tests. Error bars represented mean \pm SD. The *p*-value represented the significant difference between the E2 treated group and the E2 non-treated out of the same group, * $p < 0.05$, ** $p < 0.01$, *** $p < 1e-3$, **** $p < 1e-4$, and *ns* represented no significance. One of the three independent experiments was shown.

whereas overexpression of BAP18 showed a steady decline in AI sensitivity, and the cells became letrozole insensitive again (Fig. S7D). By influencing TFF1 eRNA expression, BAP18 is likely to significantly impact the letrozole sensitivity of MCF7 cells.

Several new therapeutic approaches have been identified that target the ER α signaling pathway against enhancer activation and have demonstrated remarkable results. By reducing the enhancer activity of many BRD4-induced genes, JQ-1, a BET-domain-containing BRD4 inhibitor, reduced breast cancer growth by dramatically inhibiting BRD4-mediated enhancer activation. Meanwhile, THZ-1, a specific CDK7 inhibitor, has been recently shown to greatly decrease MYC gene eRNA expression, thereby inhibiting ER-positive breast cancer growth. We have found that BAP18 potentially interacted with BRD4 protein in the STRING database (Fig. S7E). Under the same concentration of JQ-1 treatment, fewer BAP18-KO cells survived, and BAP18 knockout significantly improved MCF7 cell sensitivity to JQ-1 (Fig. 7F, G). In the absence of estrogen, BAP18 co-recruited on the MYC enhancer with CTCF, which explains why MCF7 cells were more sensitive to THZ-1 when BAP18 was knocked out (Fig. 7H, I). As a result of these findings, BAP18 expression was essential for the drug tolerance process in breast cancer cells, not only for the sensitivity to letrozole treatment but also for the sensitivity to enhancer inhibitors.

BAP18 is highly expressed in letrozole non-response breast cancer samples

The biological activity of BAP18 in letrozole patients was investigated using RNA-seq data collected from 58 patients taking letrozole for 7.2 months; 22 patients were classified as non-responders to letrozole and 36 patients were classified as responders to letrozole. The non-responder group exhibited greater expression of 582 genes than the responder group, suggesting that letrozole resistance might be related to these genes ($FC > 2$, $q < 1e-3$, Fig. S8A). By analyzing these highly expressed genes using Gene ontology, the data indicated that they are primarily involved in the positive regulation of intracellular estrogen receptor signaling pathway, response to the hormone, positive regulation of antibacterial peptide production, and other pathways (Fig. S8B). Our analysis of these genes revealed that they are enriched primarily in the noninfiltrating intraductal carcinoma, recurrent tumor, and estrogen receptor-positive breast cancer, all of which are implicated in these disease processes by using GO_DisGeNET (Fig. S8C). In order to explore BAP18's involvement in two critical disease pathways (Estrogen receptor positive breast cancer and Breast cancer recurrent), we found that several E2-associated genes, including *TFF1*, *CCND1*, *MYC*, and *GREB1*, were implicated in both pathways. We also found the evidences that BAP18 was highly expressed along with these genes in non-responders (Fig. 8A). According to GESA analysis, these highly expressed genes recruited and controlled by BAP18 were substantially enriched and positively correlated with in Apoptosis, cGMP-PKG signaling pathway, Ras signaling pathway,

Rap1 signaling pathway, Chemokine signaling pathway, and HIF-1 signaling pathway (Fig. S8D). The high activity of these pathways could be indicative of potential mechanisms in non-responders to AI treatment.

we collected 22 pairs of tumor tissues from breast cancer patients who received neoadjuvant endocrine therapy with letrozole (12 weeks) in order to verify the role of BAP18 in letrozole non-responders. The samples included twelve pairs of letrozole non-responders and ten pairs of letrozole responders based on PEPI. We collected RNA from sixteen pairs of these patients (eight pairs of non-responders and eight pairs of responders) for qPCR analysis. BAP18 was significantly over-expressed in the non-responders before and after AI therapy. In addition, essential genes regulated by BAP18, including *TFF1*, *GREB1*, and *MYC*, remained at a higher expression in the non-responder group following letrozole therapy, while mRNA expression of these genes was considerably decreased in the responder group (Fig. S9A). In the all-patients, *TFF1*, *GREB1*, and *MYC* mRNA expressions were positively correlated with BAP18, suggesting that BAP18 may be an important indicators for clinical letrozole sensitivity (Fig. S9B). Also, we observed a higher level of BAP18 expression in the non-responders, which was not significantly decreased following AI treatment. In contrast, BAP18 expressions were much lower among the AI responder column. A significant decrease in BAP18 expression was observed after AI treatment (Figs. 8B and S8C). According to immunohistochemical staining, BAP18 expression was significantly reduced after AI treatment in the responder group, suggesting that maintaining BAP18 expression during AI treatment may have a significant effect on AI treatment tolerance (Fig. 8C, D). As a result of these clinical evidences, BAP18 might be a potential predictor of letrozole sensitivity.

DISCUSSION

Endocrine resistance has always been a challenge in the treatment strategy for ER α -positive breast cancer patients, whose innate sensitivity to ER α signaling pathway antagonists has led to only more damaging chemotherapy or radiotherapy [53]. The fundamental mechanism of primary endocrine tolerance is assumed to be the activation of the ER α signaling pathway, which can directly alter the biological activity of tumor cells, including the regulation of cell cycle regulation, proliferation, and apoptosis of cancer cells even without estrogen [54, 55]. Here, our findings demonstrated that BAP18 significantly increased chromatin accessibility at the genome-wide level and CTCF recruitment to the enhancer regions. The increased recruitment of BAP18 and CTCF on ER α -associated enhancers significantly promoted eRNA transactivation and promoter-enhancer loop formation. Our data indicate a novel role of the BAP18/CTCF complex in regulating ER α -associated enhancer activation, suggesting that the CTCF/BAP18-mediated modulation network may act as a potential strategy for endocrine resistance in breast cancer (Fig. S10A).

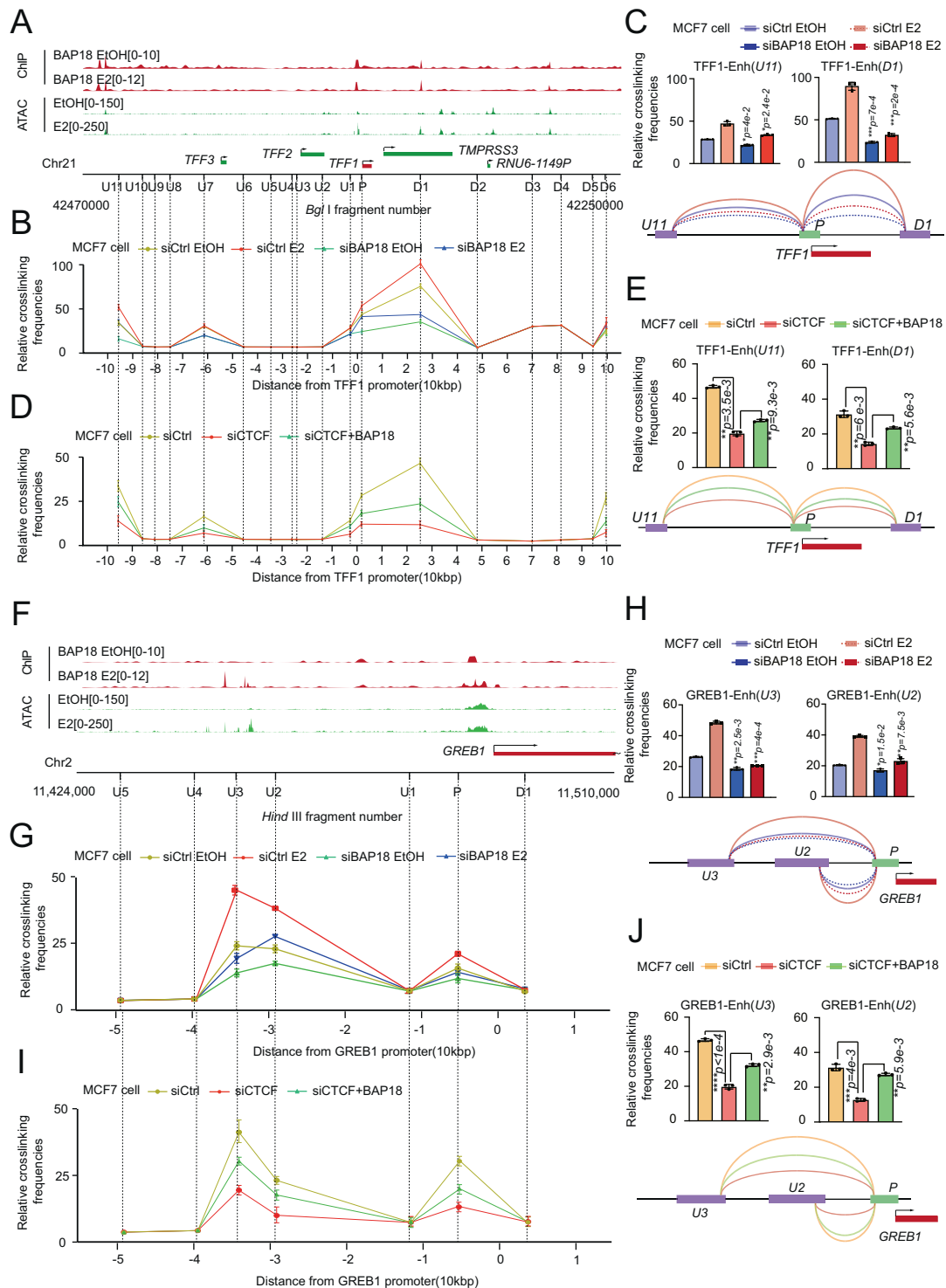
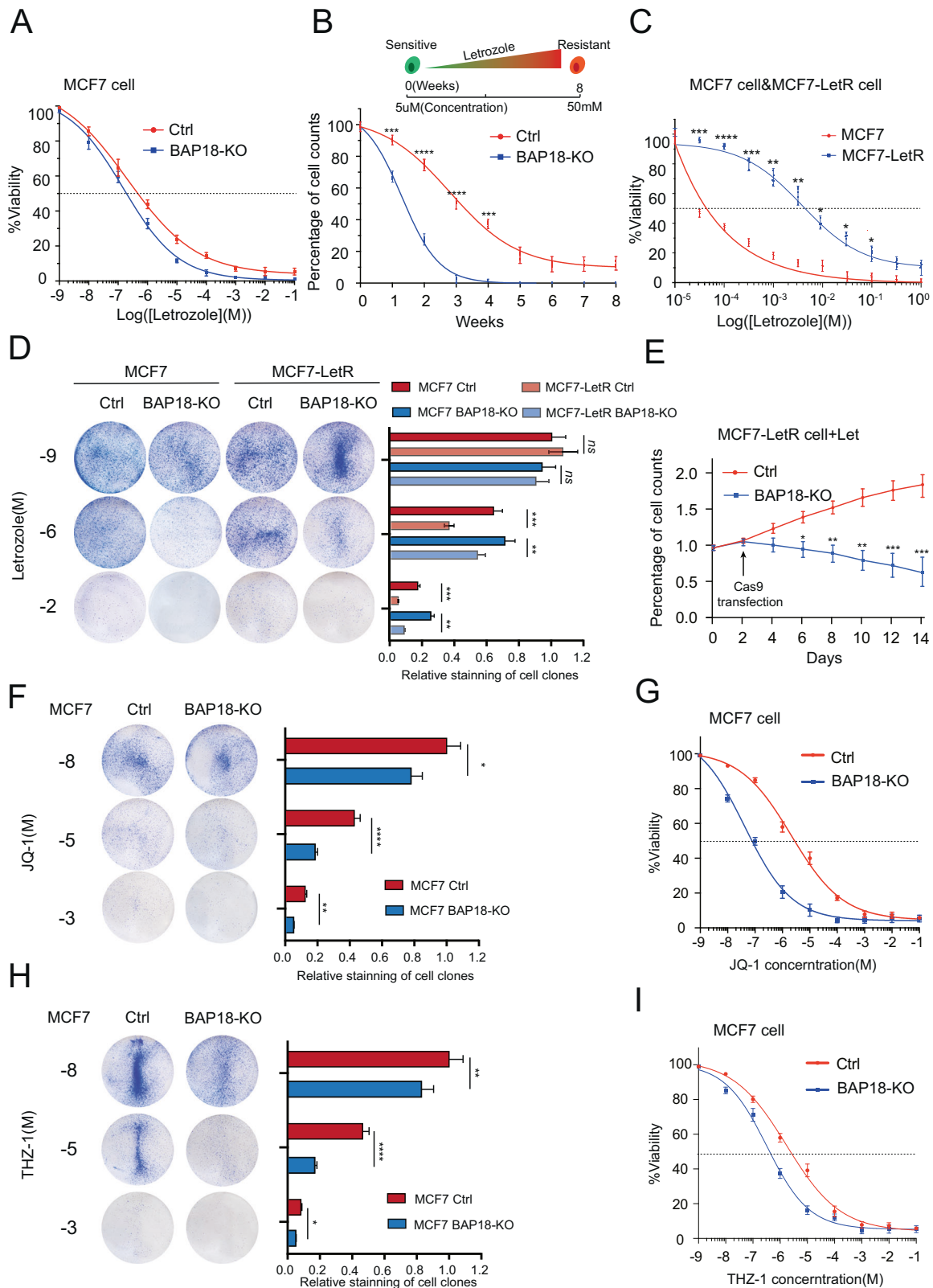


Fig. 6 BAP18 facilitates enhancer-promoter looping of E2-related genes. **A** Genome Browser showed the BAP18 recruitment peak in the *TFF1* transcript region (red) with the strength of the chromatin accessibility (green). The lower line represents the *Bgl*I enzyme digestion sites on this segment of genomic chromatin (U for upstream of the 5' promoter, and D for downstream of the 3' promoter). 3C-qPCR demonstrated the ability to crosslink between each DNA segment of *TFF1* and the promoter with BAP18 depletion under E2 treatment (**B**) or CTCF depletion without E2 treatment (**D**), and the higher the corresponding relative value represented, the more potent the ability to loop between this region and the promoter. The data was representative 3C-PCR out of three experiments. Each data point was the average of 3 groups of qPCR reactions, and error bars indicated standard error of the mean. **C**, **E** Statistical graph of the results of 3C-PCR in **B**, **D**. The height of the bars (upper panel) and the curve curvature (lower panel) size represented the relative crosslinking frequencies. **F** The Genome Browser displayed the BAP18 recruitment peak in the *GREB1* transcript area (red) and chromatin accessibility strength (green). In this section of genomic chromatin, the lower line depicts the *Hind*III enzyme digestion sites. 3C-PCR showed the relative crosslink between *Hind*III segments and promoter of *GREB1* with BAP18 depletion under E2 treatment (**G**) or CTCF depletion without E2 (**I**). **H**, **J** Statistical graph of the results of 3C-PCR in **G**, **I**.



BAP18 is required for CTCF/NURF-mediated enhancer transactivation

By modulating CTCF binding to chromatin, promoter-enhancer connection may be rewired locally and the gene expression

patterns may be altered. Chromatin remodelers are responsible for chromatin accessibility such as NuRF and SWI/SNF. As a central subunit of the SWI/SNF complex, ARID1A governed the genomic recruitment pattern of FOXA1, GATA3, and ER α through its

Fig. 7 BAP18 affects aromatase inhibitors and enhancer inhibitors in breast cancer cells. **A** The IC₅₀ experiment revealed that BAP18 deletion dramatically lowered the half-death concentration of letrozole in MCF7 cells. Cells were treated with different concentrations of letrozole for four weeks before counting the number of cells in each concentration group using cell counts. At least one of the three independent experiments was shown in the figure. **B** The graphs depicted the process of developing letrozole-resistant cells from parental MCF7 and BAP18 knockout cells (BAP18-KO). **C** The IC₅₀ assays illustrated the difference in sensitivity to letrozole between parental MCF7 cells and letrozole-resistant MCF7 cells (MCF7-LetR). **D** The cell clonal growth staining experiment revealed a significant difference in the sensitivity of MCF7 parental cells and MCF7-LetR cells to letrozole. Cultured in different concentrations of three kinds of endocrine drugs for 21 days, cells in wells were stained by R250. The right histogram uses ImageJ to count the stained area of the cell clones and *t*-tests were used. **E** The effects of short-term silencing of BAP18 in MCF7-LetR cell lines in a letrozole environment are represented with cell growth curve studies for 14 days. **F** The cell clone staining assay showed the drug sensitivity of MCF7 parental cells and BAP18 knockout cells to JQ-1. **G** The IC₅₀ assays illustrated the difference in sensitivity to letrozole between parental MCF7 cells and BAP18 depletion MCF7 cells. **H** A cell clone staining test revealed the sensitivity of MCF7 parental cells and BAP18 mutant cells to THZ-1. **I** The IC₅₀ assays exhibited the differential sensitivity to letrozole between parental MCF7 cells and BAP18 depletion MCF7 cells. All statistical tests for IC₅₀ and growth curve experiments were performed using Student *t*-tests. Error bars represented mean \pm SD, **p* < 0.05, ***p* < 0.01, ****p* < 1e-3, *****p* < 1e-4 and *ns* represented no significant. All data of cell viability and cell clone formation photographs represented one of three independent experiments.

regulatory chromatin accessibility function, allowing ER α -positive breast cancer to retain its luminal phenotype [56, 57]. Among the subunits of the NuRF complex, BPTF interacts with CTCF to influence H3 tail methylation and DNA binding in embryonic stem cells [58–60]. However, no information is available regarding the role of NuRF complex subunits in chromatin remodeling in genomic enhancers. In this study, we provided evidences to demonstrate that BAP18 consider to be the determinant protein in modulating NuRF/CTCF recruitment to enhancer. BAP18 deletion significantly weakened the interaction of NuRF subunits with CTCF and ER α (Fig. 4D). Furthermore, the depletion of BAP18 directly reduced SMARCA1 recruitment to the enhancer regions, indicating that BAP18 may be involved in coupling chromatin accessibility with enhancer transactivation (Fig. 4E). The reduced recruitment of SMARCA1 on DNA could be explained by the potent effect of BAP18 on the interactions between NuRF protein complexes. The association of BAP18 with SMARCA1 is partially depended on its N-terminal SANT domain through DNA binding. Interestingly, CTCF depletion reduced the interaction between BAP18 and SMARCA1 (Fig. S5A). The data suggested that when CTCF anchored NuRF interactions when BAP18 was recruited to CTCF binding sites, allowing the entire complex to participate more efficiently in enhancer transactivation.

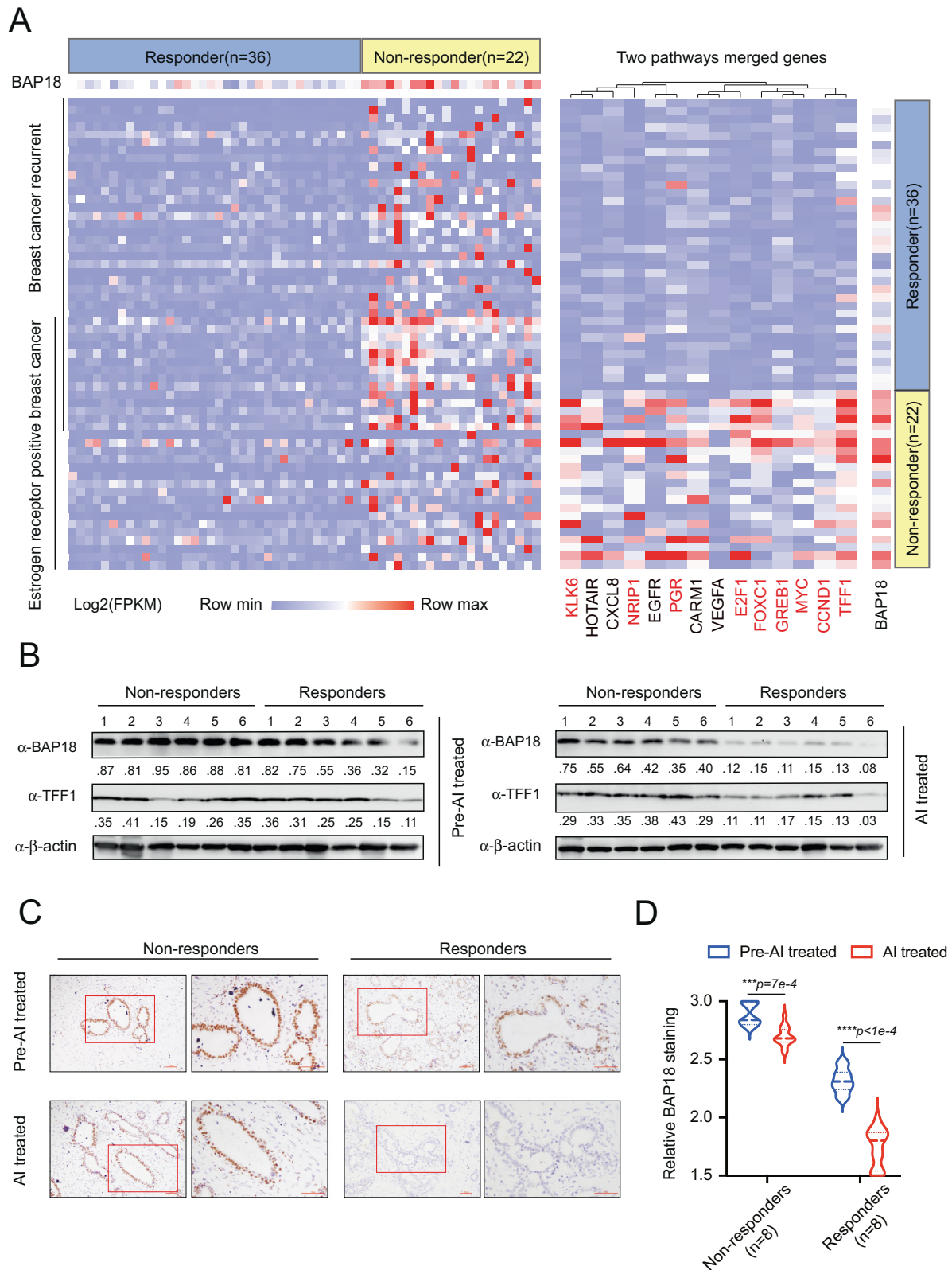
Linkage regulation of multiple genomic loci is common in ER α -associated transactivation, and dynamic chromatin remodeling has been recognized as a critical endocrine resistance mechanism [17]. ATAC-seq analysis indicates that BAP18 is also involved in the dynamic chromatin structural accessibility process as a histone H3K4me3 reader, facilitating promoter-enhancer loops of several oncogenes, such as *TFF1* and *GREB1* (Fig. 6). As a result, promoter-enhancer transcriptome activation may be an essential mechanism for preserving the expression of these oncogenes regardless of the presence of ER α . Significantly, CTCF knockdown decreased the transcriptome connectivity, and ectopic BAP18 expression reversed this reduction without estrogen treatment. The reversed connection might be related to increased chromatin accessibility by the recruitment of chromatin remodeling subunits or other proteins involved in spatial topology, including cohesins. Unlike the characteristics of promoter transcriptional activation, CTCF recruitment reflects the significance and spatiotemporal specificity of BAP18 in the transactivation process of enhancer transcriptomes. Our study proposed that BAP18 affected CTCF enhancer recruitment through the regulatory function of chromatin accessibility, providing a detailed molecular mechanism to unravel the engagement of CTCF in the ER α -mediated enhancer activation process.

BAP18 confers to endocrine resistance and other enhancer inhibitors in an E2-independent manner

A statistical analysis of gene expression of RNA-seq was conducted on AI non-responders as well as AI sensitive individuals [61]. In

addition to E2-induced genes such as *TFF1*, *MYC*, *KLK6*, *PGR*, *E2F1*, and *GREB1* (Fig. 8A), it was also discovered that the genes involved in chromatin remodeling, gene transcription, and phosphokinase activation were highly-expressed in AI non-responders (Fig. S8D). Importantly, it was found that BAP18 expression was significantly higher in non-responders than in responders after long-term treatment, suggesting that BAP18 may participate in anti-estrogen sensitivity (Fig. 8A). A number of studies have demonstrated that ER-positive breast cancers resist AI treatment through growth factor-regulated phosphorylation of signaling pathways, such as JNK, PI3K/AKT, HER2, and MAPK signaling [62–65]. It was noteworthy that BAP18-enriched active enhancers and BAP18-induced chromatin accessibility loci were occupied in the genes involved in above signaling pathways in an E2-independent manner (Figs. 1G and S2C). Mechanically, BAP18/NuRF/CTCF functioned to regulate gene eRNA transcription and E-P loops, thus contributing to AI-resistance in the absent of estrogen. A positive effect was also found in the patients receiving short-term AI treatment for 12 weeks, accompanied by a maintaining BAP18 expression (Fig. 8B–D). This maintenance of the ER α -induced gene enhancer activation was caused by the persistent high expression of BAP18, resulting in AI treatment resistance in breast cancer cells. These findings indicated that BAP18 is a potential predictor of clinical AI therapy sensitivity.

The heterogeneity and deformability of breast cancer have been the underlying cause of the development of endocrine resistance. For ER α -positive breast cancer, AI therapy is utilized as the first-line strategy, and additional pathway inhibitors are frequently used after AI tolerance [66]. Although the combination of PI3K/AKT/mTOR inhibitors or CDK4/6 inhibitors can benefit several patients, the high degree of breast cancer cell heterogeneity leads to ineffective and ultimately failure of treatment strategies for this group of advantaged individuals [61, 67, 68]. Recent studies have demonstrated that a variety of inhibitors inhibiting the enhancer activity of key genes are effective in ER-positive breast cancers such as THZ-1 and JQ-1 [69–71]. THZ-1 specific targeted CDK7, which played essential roles in gene transcription initiation and elongation [72, 73]. The *MYC* gene enhancer activity and eRNA expression could be significant inhibited by THZ-1 [74]. Here, we found that BAP18 reduction induced sensitivity of cancer cells to THZ-1, suggesting that the BAP18/CTCF could induce an enhanced *MYC* enhancer activity under an E2-independent condition that resulted in THZ-1 insensitivity (Fig. 7F, G). BRD4 could be inhibited by JQ-1 as a critical transcriptional coactivator of ER α . BRD4 enhanced transcription of genes containing EREs on enhancers or super-enhancers of genes such as *MYC*, *IRF4*, *CCND1*, and *BCL2L1* [75, 76]. Similarly, BAP18-KO significantly increased JQ-1 sensitivity as a result of an potential interplay between BAP18 and BRD4-mediated enhancer activation (Fig. 7H, I). In patients with high levels of BAP18, BAP18 activated the eRNA transcription targeted



by CTCF/NuRF (*MYC* enhancers) or cross-talked with BRD4 (BRD4-targeted enhancers), thus inducing a drug resistance. Based on these results, BAP18 expression might be used to predict breast cancer cell response to two enhancer inhibitors.

The analysis of ChIP-seq and ATAC-seq data provided a comprehensive basis for understanding how BAP18 influences genome-wide chromatin remodeling and enhancer activation. Our work may provide further insight into the potential strategies to

Fig. 8 BAP18 is highly expressed in letrozole non-response patients. **A** The differential expression of genes in the two signaling pathways was shown in a heat map of RNA-seq data in 36 responders and 22 non-responders. The right panel displayed the expression patterns of genes which were engaged in both pathways in all patients. The colors of the blocks were displayed relative to \log_2 (FPKM) values. **B** The findings of western blot experiments revealed the levels of expression of BAP18 and TFF1 proteins in 12 patients (6 non-responders and 6 responders), representing the magnitude of the grayscale values relative to β -actin. Numerical values showing the degree of staining of BAP18 relative to the internal reference (β -actin), using ImageJ for quantitative statistics. **C** Immunohistochemical staining demonstrates the expression of BAP18 staining in tumors of AI non-responders and AI responders before and after AI treatment, respectively. Each group shows staining of breast luminal at 10 \times (left) and 20 \times (right) with a scale size of 100 μ m. **D** The violin box plot shows the statistical results of immunohistochemistry and the relative BAP18 staining scoring criteria written in the material and methods section.

overcome endocrine resistance and discover novel epigenetically therapeutic targets.

DATA AVAILABILITY

The data and material that support the findings of this study are available from the corresponding author upon reasonable request.

REFERENCES

- Husemann Y, Geigl JB, Schubert F, Musiani P, Meyer M, Burghart E, et al. Systemic spread is an early step in breast cancer. *Cancer Cell*. 2008;13:58–68.
- Bray F, Ferlay J, Soerjomataram I, Siegel RL, Torre LA, Jemal A. Global cancer statistics 2018: GLOBOCAN estimates of incidence and mortality worldwide for 36 cancers in 185 countries. *CA Cancer J Clin*. 2018;68:394–424.
- Koren S, Bentires-Alj M. Breast Tumor Heterogeneity: Source of Fitness, Hurdle for Therapy. *Mol Cell*. 2015;60:537–46.
- Cardoso F, Paluch-Shimon S, Senkus E, Curigliano G, Aapro MS, Andre F, et al. 5th ESO-ESMO international consensus guidelines for advanced breast cancer (ABC 5). *Ann Oncol*. 2020;31:1623–49.
- Harbeck N, Gnant M. Breast cancer. *Lancet*. 2017;389:1134–50.
- Chen S. An “omics” approach to determine the mechanisms of acquired aromatase inhibitor resistance. *OMICS*. 2011;15:347–52.
- Cardoso F, Costa A, Senkus E, Aapro M, Andre F, Barrios CH, et al. 3rd ESO-ESMO International Consensus Guidelines for Advanced Breast Cancer (ABC 3). *Ann Oncol*. 2017;28:16–33.
- Early Breast Cancer Trialists’ Collaborative G, Davies C, Godwin J, Gray R, Clarke M, Cutter D, et al. Relevance of breast cancer hormone receptors and other factors to the efficacy of adjuvant tamoxifen: patient-level meta-analysis of randomised trials. *Lancet*. 2011;378:771–84.
- Toy W, Shen Y, Won H, Green B, Sakr RA, Will M, et al. ESR1 ligand-binding domain mutations in hormone-resistant breast cancer. *Nat Genet*. 2013;45:1439–45.
- Zwart W, Griekspoor A, Berno V, Lakeman K, Jalink K, Mancini M, et al. PKA-induced resistance to tamoxifen is associated with an altered orientation of ERalpha towards co-activator SRC-1. *EMBO J*. 2007;26:3534–44.
- Kastrati I, Semina S, Gordon B, Smart E. Insights into how phosphorylation of estrogen receptor at serine 305 modulates tamoxifen activity in breast cancer. *Mol Cell Endocrinol*. 2019;483:97–101.
- Servetto A, Formisano L, Arteaga CL. FGFR signaling and endocrine resistance in breast cancer: Challenges for the clinical development of FGFR inhibitors. *Biochim Biophys Acta Rev Cancer*. 2021;1876:188595.
- Sklias A, Halaburkova A, Vanzan L, Jimenez NF, Cuenin C, Bouaoun L, et al. Epigenetic remodelling of enhancers in response to estrogen deprivation and re-stimulation. *Nucl Acids Res*. 2021;49:9738–54.
- Escher TE, Dandawate P, Sayed A, Hagan CR, Anant S, Lewis-Wambi J. Enhanced IFNalpha Signaling Promotes Ligand-Independent Activation of ERalpha to Promote Aromatase Inhibitor Resistance in Breast Cancer. *Cancers (Basel)* 2021;13.
- Le Romancer M, Poulard C, Cohen P, Sentis S, Renoir JM, Corbo L. Cracking the estrogen receptor’s posttranslational code in breast tumors. *Endocr Rev*. 2011;32:597–622.
- Jeselsohn R, De Angelis C, Brown M, Schiff R. The Evolving Role of the Estrogen Receptor Mutations in Endocrine Therapy-Resistant Breast Cancer. *Curr Oncol Rep*. 2017;19:35.
- Zhou Y, Gerrard DL, Wang J, Li T, Yang Y, Fritz AJ, et al. Temporal dynamic reorganization of 3D chromatin architecture in hormone-induced breast cancer and endocrine resistance. *Nat Commun*. 2019;10:1522.
- Fridriksdottir AJ, Kim J, Villadsen R, Klitgaard MC, Hopkinson BM, Petersen OW, et al. Propagation of oestrogen receptor-positive and oestrogen-responsive normal human breast cells in culture. *Nat Commun*. 2015;6:8786.
- Holding AN, Cullen AE, Markowitz F. Genome-wide Estrogen Receptor-alpha activation is sustained, not cyclical. *Elife* 2018;7.
- Li W, Notani D, Ma Q, Tanasa B, Nunez E, Chen AY, et al. Functional roles of enhancer RNAs for oestrogen-dependent transcriptional activation. *Nature*. 2013;498:516–20.
- Pnueli L, Rudnizky S, Yosefzon Y, Melamed P. RNA transcribed from a distal enhancer is required for activating the chromatin at the promoter of the gonadotropin alpha-subunit gene. *Proc Natl Acad Sci*. 2015;112:4369–74.
- Liu Z, Merkurjev D, Yang F, Li W, Oh S, Friedman MJ, et al. Enhancer activation requires trans-recruitment of a mega transcription factor complex. *Cell*. 2014;159:358–73.
- Zhu C, Li L, Zhang Z, Bi M, Wang H, Su W, et al. A Non-canonical Role of YAP/TEAD Is Required for Activation of Estrogen-Regulated Enhancers in Breast Cancer. *Mol Cell*. 2019;75:791–806.e798.
- Achinger-Kawecka J, Valdes-Mora F, Luu PL, Giles KA, Caldon CE, Qu W, et al. Epigenetic reprogramming at estrogen-receptor binding sites alters 3D chromatin landscape in endocrine-resistant breast cancer. *Nat Commun*. 2020;11:320.
- Watson G, Ronai ZA, Lau E. ATF2, a paradigm of the multifaceted regulation of transcription factors in biology and disease. *Pharm Res*. 2017;119:347–57.
- Huebner K, Prochazka J, Monteiro AC, Mahadevan V, Schneider-Stock R. The activating transcription factor 2: an influencer of cancer progression. *Mutagenesis*. 2019;34:375–89.
- Pugacheva EM, Kubo N, Loukinov D, Tajmull M, Kang S, Kovalchuk AL, et al. CTCF mediates chromatin looping via N-terminal domain-dependent cohesin retention. *Proc Natl Acad Sci*. 2020;117:2020–31.
- Quintin J, Le Peron C, Palierne G, Bizot M, Cunha S, Serandour AA, et al. Dynamic estrogen receptor interactomes control estrogen-responsive trefoil Factor (TFF) locus cell-specific activities. *Mol Cell Biol*. 2014;34:2418–36.
- Ross-Innes CS, Brown GD, Carroll JS. A co-ordinated interaction between CTCF and ER in breast cancer cells. *BMC Genomics*. 2011;12:593.
- Korkmaz G, Manber Z, Lopes R, Prekovic S, Schuurman K, Kim Y, et al. A CRISPR-Cas9 screen identifies essential CTCF anchor sites for estrogen receptor-driven breast cancer cell proliferation. *Nucl Acids Res*. 2019;47:9557–72.
- Razavi P, Chang MT, Xu G, Bandlamudi C, Ross DS, Vasan N, et al. The Genomic Landscape of Endocrine-Resistant Advanced Breast Cancers. *Cancer Cell*. 2018;34:427–38.e426.
- Fiorito E, Sharma Y, Gifillan S, Wang S, Singh SK, Satheesh SV, et al. CTCF modulates Estrogen Receptor function through specific chromatin and nuclear matrix interactions. *Nucl Acids Res*. 2016;44:10588–602.
- Arnesen S, Blanchard Z, Williams MM, Berrett KC, Li Z, Oesterreich S, et al. Estrogen Receptor Alpha Mutations in Breast Cancer Cells Cause Gene Expression Changes through Constant Activity and Secondary Effects. *Cancer Res*. 2021;81:539–51.
- Barbaric S, Reinke H, Horz W. Multiple mechanistically distinct functions of SAGA at the PHO5 promoter. *Mol Cell Biol*. 2003;23:3468–76.
- Boyer LA, Langer MR, Crowley KA, Tan S, Denu JM, Peterson CL. Essential role for the SANT domain in the functioning of multiple chromatin remodeling enzymes. *Mol Cell*. 2002;10:935–42.
- Sterner DE, Wang X, Bloom MH, Simon GM, Berger SL. The SANT domain of Ada2 is required for normal acetylation of histones by the yeast SAGA complex. *J Biol Chem*. 2002;277:8178–86.
- Vermeulen M, Eberl HC, Matarese F, Marks H, Denisov S, Butter F, et al. Quantitative interaction proteomics and genome-wide profiling of epigenetic histone marks and their readers. *Cell*. 2010;142:967–80.
- Sun S, Zhong X, Wang C, Sun H, Wang S, Zhou T, et al. BAP18 coactivates androgen receptor action and promotes prostate cancer progression. *Nucl Acids Res*. 2016;44:8112–28.
- Wang X, Wang C, Yan G, Kang Y, Sun G, Wang S, et al. BAP18 is involved in upregulation of CCND1/2 transcription to promote cell growth in oral squamous cell carcinoma. *EBioMedicine*. 2020;53:102685.
- Sun G, Wang C, Wang S, Sun H, Zeng K, Zou R, et al. An H3K4me3 reader, BAP18 as an adaptor of COMPASS-like core subunits co-activates ERalpha action and associates with the sensitivity of antiestrogen in breast cancer. *Nucl Acids Res*. 2020;48:10768–84.

41. Tang T, Jiao J, Li D, Sun G, Lin L, Wang C, et al. The function of BAP18 on modulation of androgen receptor action in luteinized granulosa cells from normal weight women with and without PCOS. *Mol Cell Endocrinol*. 2021;527:111228.
42. Wei SJ, Li J, Wang JY, Zhang LX, Zhang HB, Du DJ, et al. BAP18 induces growth of non-small-cell lung carcinoma through upregulating transcriptional level of CCND1/2. *Eur Rev Med Pharm Sci*. 2022;26:3074–82.
43. Zhang YL, Deng L, Liao L, Yang SY, Hu SY, Ning Y, et al. Chromatin complexes subunit BAP18 promotes triple-negative breast cancer progression through transcriptional activation of oncogene S100A9. *Cell Death Dis*. 2022;13:408.
44. Cong L, Ran FA, Cox D, Lin S, Barretto R, Habib N, et al. Multiplex genome engineering using CRISPR/Cas systems. *Science*. 2013;339:819–23.
45. Wang C, Sun H, Zou R, Zhou T, Wang S, Sun S, et al. MDC1 functionally identified as an androgen receptor co-activator participates in suppression of prostate cancer. *Nucl Acids Res*. 2015;43:4893–908.
46. Nelson JD, Denisenko O, Bomsztyk K. Protocol for the fast chromatin immunoprecipitation (ChIP) method. *Nat Protoc*. 2006;1:179–85.
47. Muthurajan U, Mattioli F, Bergeron S, Zhou K, Gu Y, Chakravarthy S, et al. In Vitro Chromatin Assembly: Strategies and Quality Control. *Methods Enzymol*. 2016;573:3–41.
48. Hagege H, Klous P, Braem C, Splinter E, Dekker J, Cathala G, et al. Quantitative analysis of chromosome conformation capture assays (3C-qPCR). *Nat Protoc*. 2007;2:1722–33.
49. Lee KM, Guerrero-Zotano AL, Servetto A, Sudhan DR, Lin CC, Formisano L, et al. Proline rich 11 (PRR11) overexpression amplifies PI3K signaling and promotes antiestrogen resistance in breast cancer. *Nat Commun*. 2020;11:5488.
50. Kong SL, Li G, Loh SL, Sung WK, Liu ET. Cellular reprogramming by the conjoint action of ERalpha, FOXA1, and GATA3 to a ligand-inducible growth state. *Mol Syst Biol*. 2011;7:526.
51. Theodorou V, Stark R, Menon S, Carroll JS. GATA3 acts upstream of FOXA1 in mediating ESR1 binding by shaping enhancer accessibility. *Genome Res*. 2013;23:12–22.
52. Tan Y, Jin C, Ma W, Hu Y, Tanasa B, Oh S, et al. Dismissal of RNA Polymerase II Underlies a Large Ligand-Induced Enhancer Decommissioning Program. *Mol Cell*. 2018;71:526–39.e528.
53. Miranda F, Prazeres H, Mendes F, Martins D, Schmitt F. Resistance to endocrine therapy in HR + and/or HER2 + breast cancer: the most promising predictive biomarkers. *Mol Biol Rep*. 2022;49:717–33.
54. Fu X, De Angelis C, Schiff R. Interferon Signaling in Estrogen Receptor-positive Breast Cancer: A Revitalized Topic. *Endocrinology* 2022;163.
55. Xu XQ, Pan XH, Wang TT, Wang J, Yang B, He QJ, et al. Intrinsic and acquired resistance to CDK4/6 inhibitors and potential overcoming strategies. *Acta Pharm Sin*. 2021;42:171–8.
56. Xu G, Chhangawala S, Cocco E, Razavi P, Cai Y, Otto JE, et al. ARID1A determines luminal identity and therapeutic response in estrogen-receptor-positive breast cancer. *Nat Genet*. 2020;52:198–207.
57. Nagarajan S, Rao SV, Sutton J, Cheeseman D, Dunn S, Papachristou EK, et al. ARID1A influences HDAC1/BRD4 activity, intrinsic proliferative capacity and breast cancer treatment response. *Nat Genet*. 2020;52:187–97.
58. Qiu Z, Song C, Malakouti N, Murray D, Hariz A, Zimmerman M, et al. Functional interactions between NURF and Ctf regulate gene expression. *Mol Cell Biol*. 2015;35:224–37.
59. Wysocka J, Swigut T, Xiao H, Milne TA, Kwon SY, Landry J, et al. A PHD finger of NURF couples histone H3 lysine 4 trimethylation with chromatin remodelling. *Nature*. 2006;442:86–90.
60. Zahid H, Buchholz CR, Singh M, Ciccone MF, Chan A, Nithianantham S, et al. New Design Rules for Developing Potent Cell-Active Inhibitors of the Nucleosome Remodeling Factor (NURF) via BPTF Bromodomain Inhibition. *J Med Chem*. 2021;64:13902–17.
61. Guerrero-Zotano AL, Stricker TP, Formisano L, Hutchinson KE, Stover DG, Lee KM, et al. ER(+) Breast Cancers Resistant to Prolonged Neoadjuvant Letrozole Exhibit an E2F4 Transcriptional Program Sensitive to CDK4/6 Inhibitors. *Clin Cancer Res*. 2018;24:2517–29.
62. Griffiths JI, Chen J, Cosgrove PA, O'Dea A, Sharma P, Ma C, et al. Serial single-cell genomics reveals convergent subclonal evolution of resistance as early-stage breast cancer patients progress on endocrine plus CDK4/6 therapy. *Nat Cancer*. 2021;2:658–71.
63. Walker RR, Patel JR, Gupta A, Davidson AM, Williams CC, Payton-Stewart F, et al. Glycollins Trigger Anti-Proliferative Effects in Hormone-Dependent Aromatase-Inhibitor-Resistant Breast Cancer Cells through the Induction of Apoptosis. *Int J Mol Sci*. 2022;23.
64. Sharifi MN, Anandan A, Grogan P, O'Regan RM. Therapy after cyclin-dependent kinase inhibition in metastatic hormone receptor-positive breast cancer: Resistance mechanisms and novel treatment strategies. *Cancer*. 2020;126:3400–16.
65. Jansen VM, Bhola NE, Bauer JA, Formisano L, Lee KM, Hutchinson KE, et al. Kinome-Wide RNA Interference Screen Reveals a Role for PDK1 in Acquired Resistance to CDK4/6 Inhibition in ER-Positive Breast Cancer. *Cancer Res*. 2017;77:2488–99.
66. Miller CA, Gindin Y, Lu C, Griffith OL, Griffith M, Shen D, et al. Aromatase inhibition remodels the clonal architecture of estrogen-receptor-positive breast cancers. *Nat Commun*. 2016;7:12498.
67. Wardell SE, Ellis MJ, Alley HM, Eisele K, VanArsdale T, Dann SG, et al. Efficacy of SERD/SERM Hybrid-CDK4/6 Inhibitor Combinations in Models of Endocrine Therapy-Resistant Breast Cancer. *Clin Cancer Res*. 2015;21:5121–30.
68. Kirkegaard T, Witton CJ, McGlynn LM, Tovey SM, Dunne B, Lyon A, et al. AKT activation predicts outcome in breast cancer patients treated with tamoxifen. *J Pathol*. 2005;207:139–46.
69. McDermott MSJ, Sharko AC, Munie J, Kassler S, Melendez T, Lim CU, et al. CDK7 Inhibition is Effective in all the Subtypes of Breast Cancer: Determinants of Response and Synergy with EGFR Inhibition. *Cells* 2020;9.
70. Attia YM, Shouman SA, Salama SA, Ivan C, Elsayed AM, Amero P, et al. Blockade of CDK7 Reverses Endocrine Therapy Resistance in Breast Cancer. *Int J Mol Sci*. 2020;21.
71. Sahni JM, Keri RA. Targeting bromodomain and extraterminal proteins in breast cancer. *Pharm Res*. 2018;129:156–76.
72. Akhtar MS, Heidemann M, Tietjen JR, Zhang DW, Chapman RD, Eick D, et al. FTIIH kinase places bivalent marks on the carboxy-terminal domain of RNA polymerase II. *Mol Cell*. 2009;34:387–93.
73. Larochelle S, Amat R, Glover-Cutter K, Sanso M, Zhang C, Allen JJ, et al. Cyclin-dependent kinase control of the initiation-to-elongation switch of RNA polymerase II. *Nat Struct Mol Biol*. 2012;19:1108–15.
74. Zeng M, Kwiatkowski NP, Zhang T, Nabet B, Xu M, Liang Y, et al. Targeting MYC dependency in ovarian cancer through inhibition of CDK7 and CDK12/13. *Elife* 2018;7.
75. Loven J, Hoke HA, Lin CY, Lau A, Orlando DA, Vakoc CR, et al. Selective inhibition of tumor oncogenes by disruption of super-enhancers. *Cell*. 2013;153:320–34.
76. Chapuy B, McKeown MR, Lin CY, Monti S, Roemer MG, Qi J, et al. Discovery and characterization of super-enhancer-associated dependencies in diffuse large B cell lymphoma. *Cancer Cell*. 2013;24:777–90.

ACKNOWLEDGEMENTS

We thank Professor Kato Shigeaki from center of regional cooperation in Iwaki Meisei University for his important discussion and support. We appreciate Dr. Yunlong Huo and Dr. Fang Dong for their excellent technical assistance. We thank SeqHealth Tech Co., Ltd Wuhan, China, for ChIP-seq and ATAC-seq analysis.

AUTHOR CONTRIBUTIONS

Conceptualization: GS and YZ. Methodology: GS. Software: YB, HL and MH. Validation: CW and YZ. Formal analysis: GS and YZ. Investigation: GS, BZ, MW, RL, DZ and SW. Resources: YW, SW, KZ, SL, and LL. Writing: GS and YZ. Supervision: QZ and YZ.

FUNDING

This study was supported by the National Natural Science Foundation of China (32170603, 31871286 for YZ, 81872015, 82273123 for CW, 32100440 for GS); China Postdoctoral Science Foundation (276066) for GS; Foundation of Liaoning Province of China (LJKZ0756 for Shengli Wang); Local projects supported by the central government (2022JH6/100100035 for YZ); Foreign expert project of Ministry of Science and Technology (G2022006007L for YZ).

COMPETING INTERESTS

The authors declare no competing interests.

ETHICS

Our study makes use of publicly available sequencing datasets as cited in the results section. As such, prior ethics approval has been obtained for these studies and no additional approval is required. All primary breast cancer tissues and adjacent tissues of patients were procured from the Liaoning Cancer Hospital of China Medical University, all of which received permission from patients already.

ADDITIONAL INFORMATION

Supplementary information The online version contains supplementary material available at <https://doi.org/10.1038/s41418-023-01135-y>.

Correspondence and requests for materials should be addressed to Yue Zhao.

Reprints and permission information is available at <http://www.nature.com/reprints>

Publisher's note Springer Nature remains neutral with regard to jurisdictional claims in published maps and institutional affiliations.

Springer Nature or its licensor (e.g. a society or other partner) holds exclusive rights to this article under a publishing agreement with the author(s) or other rightsholder(s); author self-archiving of the accepted manuscript version of this article is solely governed by the terms of such publishing agreement and applicable law.